"Radiation hardness studies of semiconductor detectors exposed to a low dose irradiation of accelerated ions in MeV energy range"

Zeljko Pastuovic
Centre for Accelerator Science
Australian Nuclear Science and Technology Organisation (ANSTO)
zkp@ansto.gov.au

INTERNATIONAL CONFERENCE ON APPLICATIONS OF NUCLEAR TECHNIQUES - CRETE17, 16th June2017

Outline

1. **ANSTO – Nucl. Sci. & Tech. Landmark Infrastructure -**

   Centre for Accelerator Science – SIRIUS 6 MV system

2. **Particle detection by semiconductor detectors**
   - Basics: MeV ion-matter interaction; low vs high damage regimes
   - Pristine vs used (partly damaged) detector
   - Experimental protocol – “single ion” implantation using the nuclear microprobe
   - Model to interpret performance of partly damaged detectors
   - Results –validation of the model using silicon detectors
3. **Overview of recent 4H-SiC related work**
   - Effects on doping - CV
   - Effects on carrier capture & charge collection - IBIC
   - Deep defect characterisation - DLTS
4. **Conclusions**
5. **Acknowledgements**

ANSTO Lucas Heights Campus

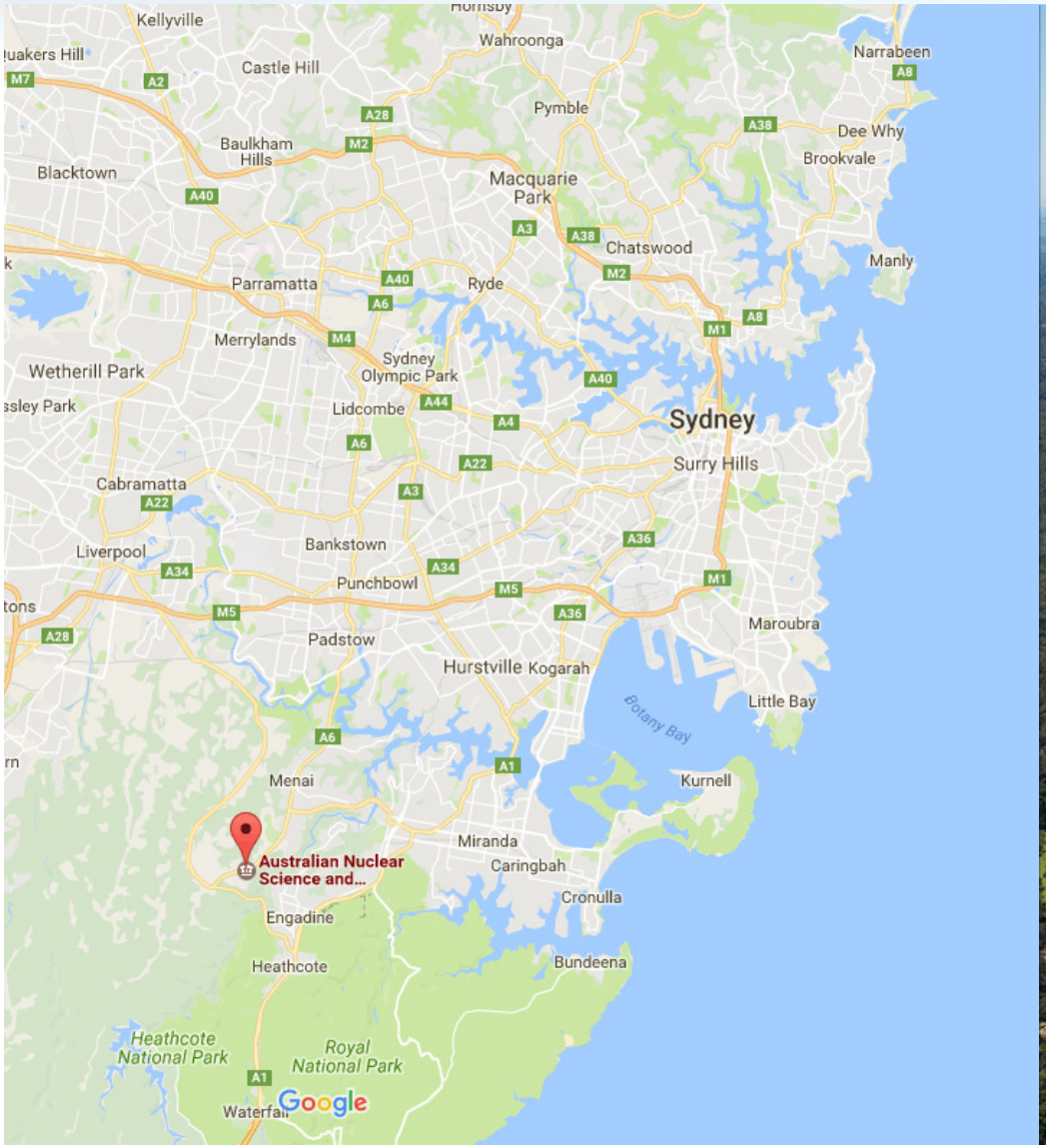

Nuclear Sci. & Tech. Landmark Infrastructure

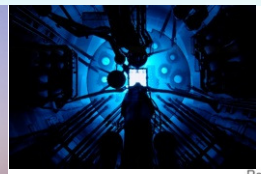

Australian Synchrotron

http://www.synchrotron.org.au/

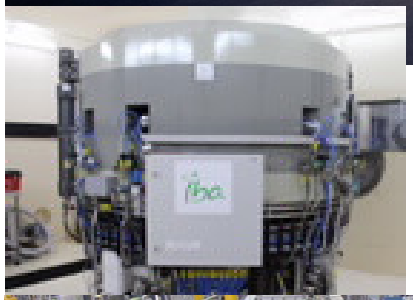

Camperdown Cyclotron

OPAL Research Reactor

http://www.ansto.gov.au/AboutANSTO/OPAL/index.htm

Australian Centre for Neutron Scattering

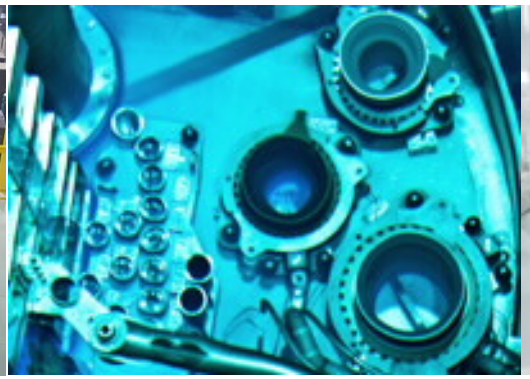

Neutron Activation Facility

National Deuteration Facility

Centre for Accelerator Science

Centre for Accelerator Science (CAS)

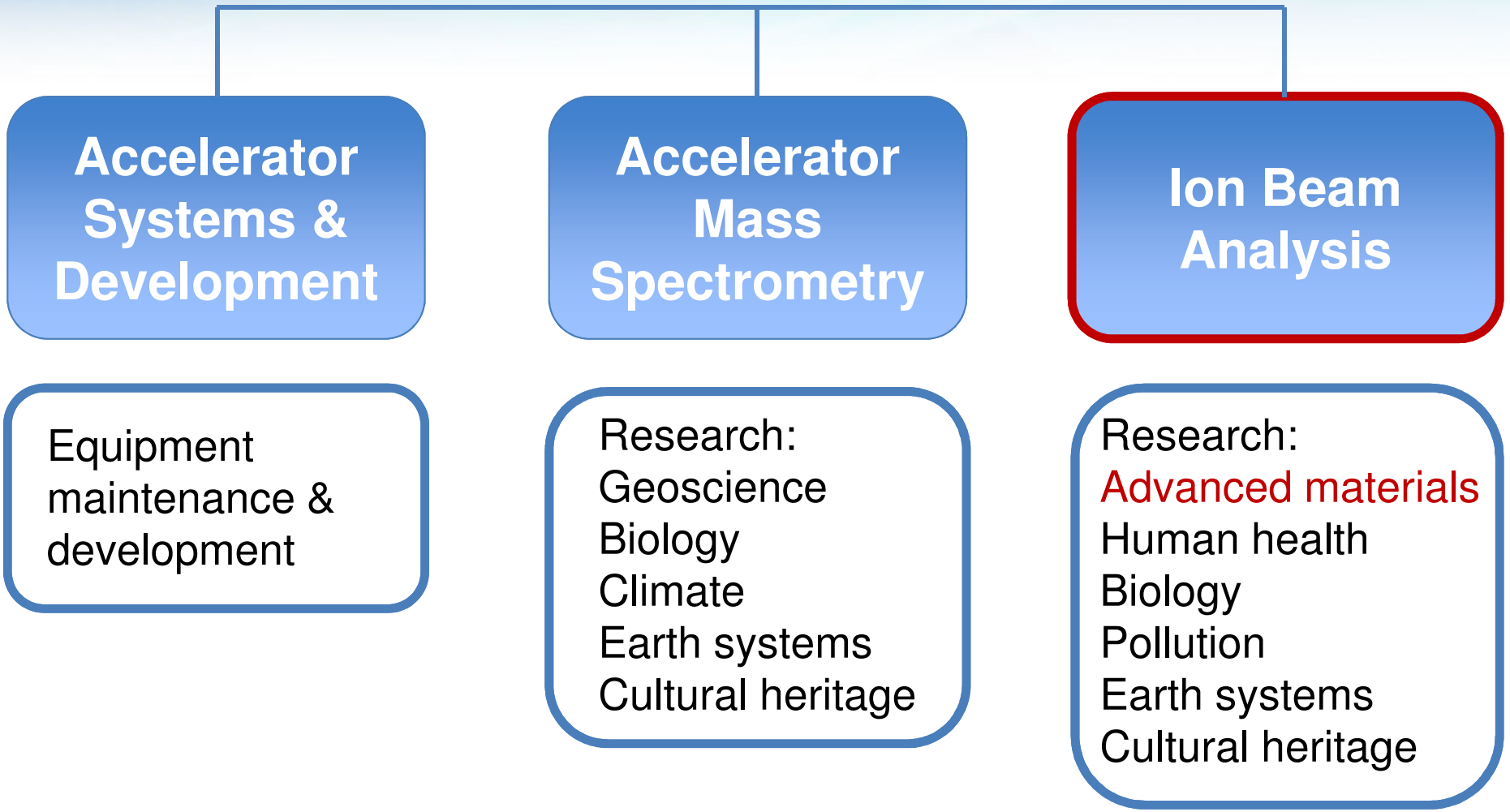

Advanced materials research @ CAS

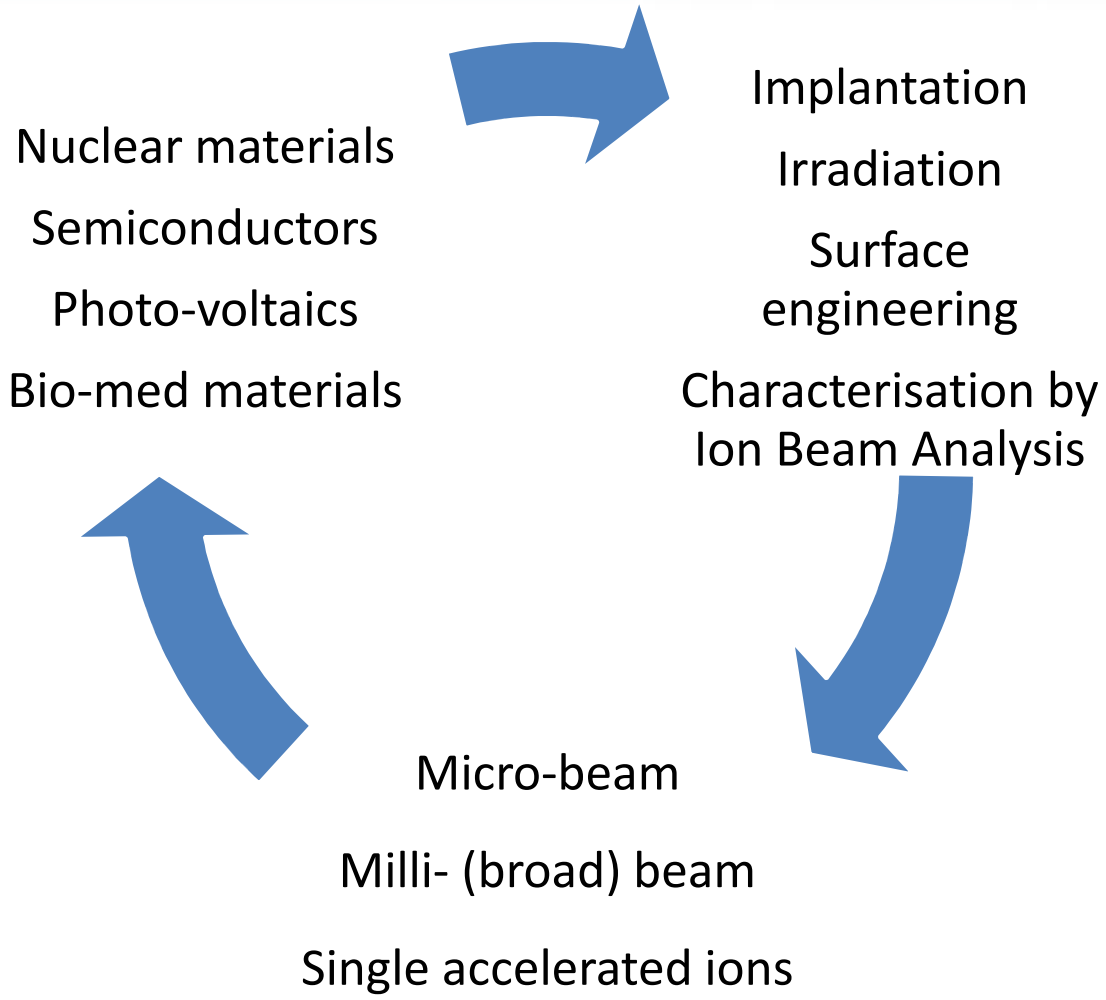

Accelerator Systems @ CAS

SIRIUS (6 MV NEC 18 SHD-2 Tandem Pelletron 2015)

VEGA (1 MV NEC Tandem - Pelletron 2014)

http://www.ansto.gov.au/ResearchHub/OurInfrastructure/acceleratorsciencecentre/index.htm

STAR (2 MV HVEE Tandetron 2003)

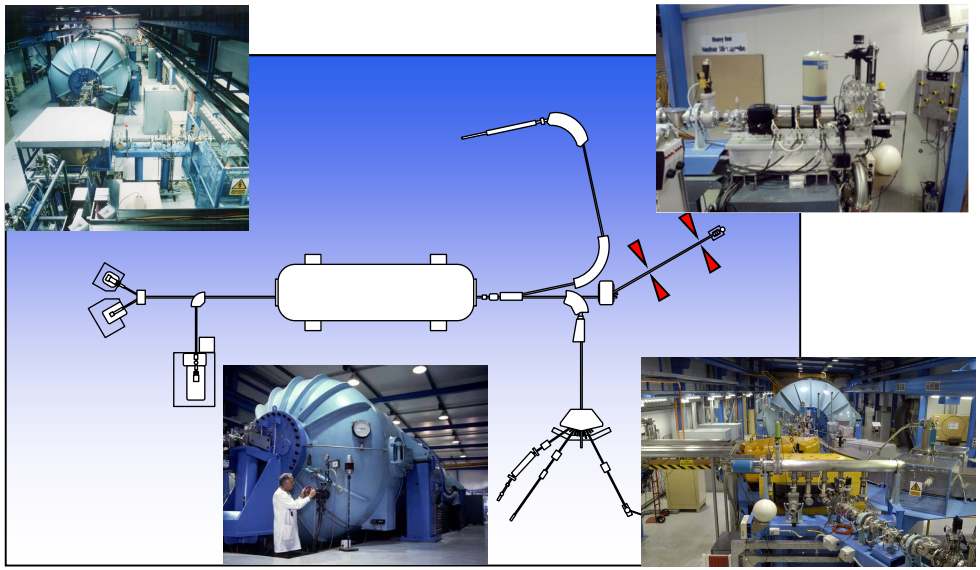

ANTARES (10 MV HVE FN Tandem - Pelletron 1998)

SIRIUS Nuclear Microprobe

- **Aim:**

  - IBA microscopy for elemental characterisation of sample surfaces and near surface regions

  - material modification by single-ion implantation or rarefied ion microbeam irradiation with sub-μm resolution

- **Capabilities:**
  - **Ion beam focusing up to ME/q^2=39 amu MeV/e^2**
  - **Microprobe focusing system: OM - 150 triplet**
  - **Beam spot size of 1-2 μm or better**
  - **"Dog – leg" beam scanning 2 × 2 mm^2: OM – 26**
  - **Beam blanking**
  - **Target positioning/scanning w nm resolution**
  - **Automated object and collimating slits**

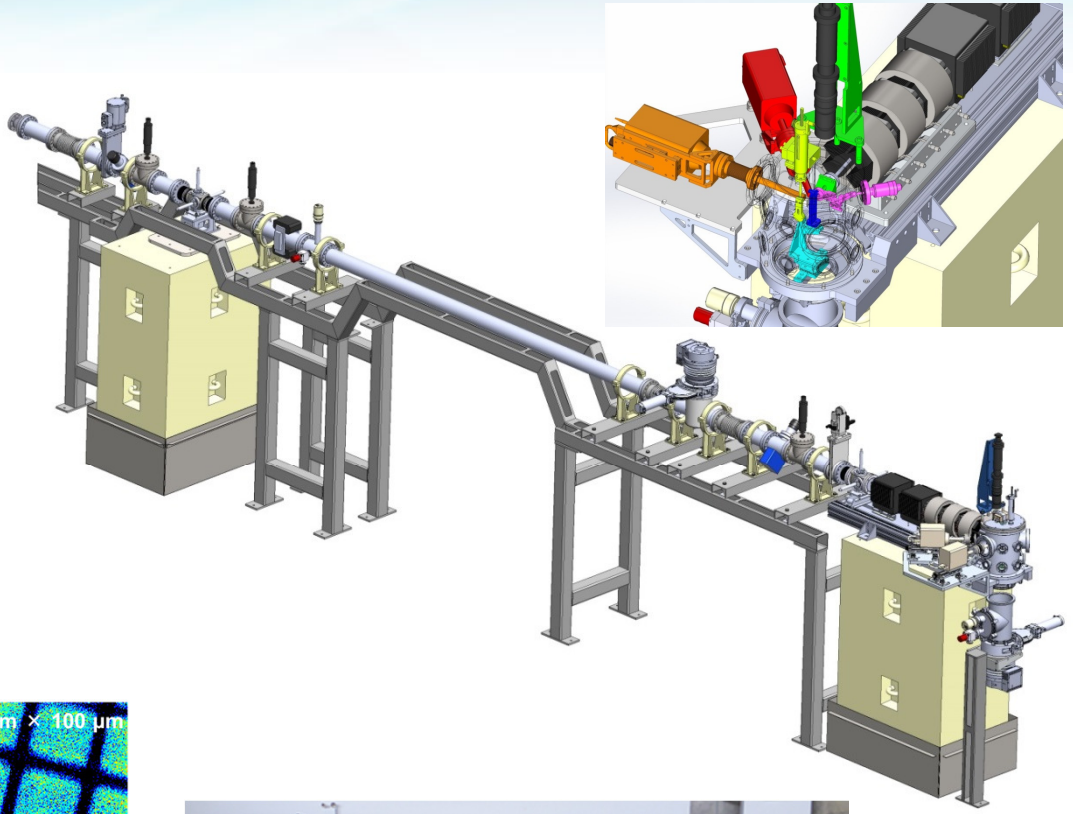

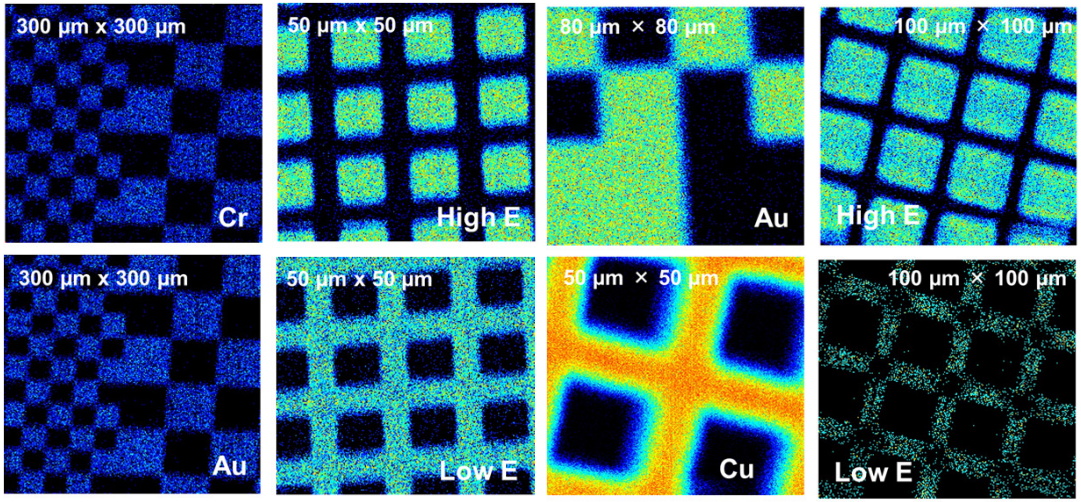

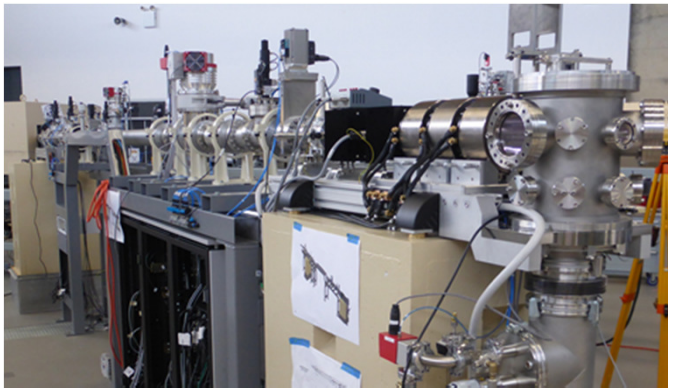

Methodology: Ion implantation in the “single ion” regime in planar SC device

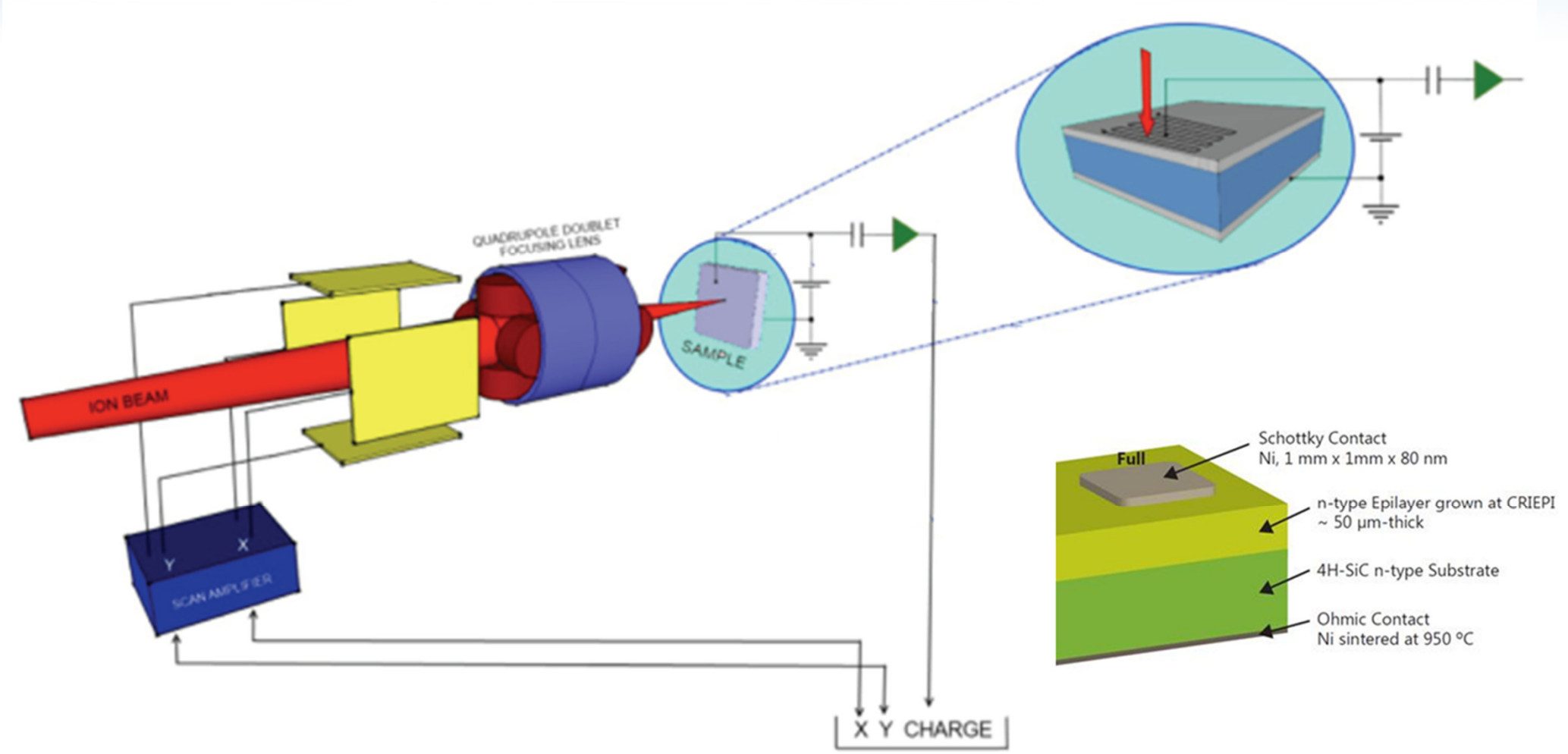

Schematics of the nuclear microprobe setup for patterned ion implantation of 4H-SiC Schottky barrier diode samples using a fast-scanning reduced-rate microbeam and IBIC microscopy for single ion detection.

What and why we do it?

➢ **FOCUS: detailed study of the low level radiation damage in semiconductor devices**

➢ Radiation induced effects on the structural, mechanical and electrical properties of materials has been studied for almost 50 years → significant gaps in the understanding of:

❖ **What types of defects are formed under specific irradiation conditions**?

✓ **How they can be characterised**?

✓ **What is their influence on the performance of irradiated devices**?

➢ This lack of understanding is particularly important for damage caused by **ions heavier than protons and ion energies in the keV to MeV range**

➢ **OBJECTIVES:**

✓ ***Establish the experimental protocol suitable for studies***

✓ ***Develop robust model for interpretation of ion beam induced effects on performance of SC devices***

Unique property of accelerated ions – TUNABLE PARTICLE RANGE

Accelerators:
Terminal voltages – 0.3 to 6 MV
Ion sources – sputtering,
RF alphatross, duoplasmatron (Z_{ion} = 1 – 82)

Good selection of FIB ranges !! →
material scientist dream come true!

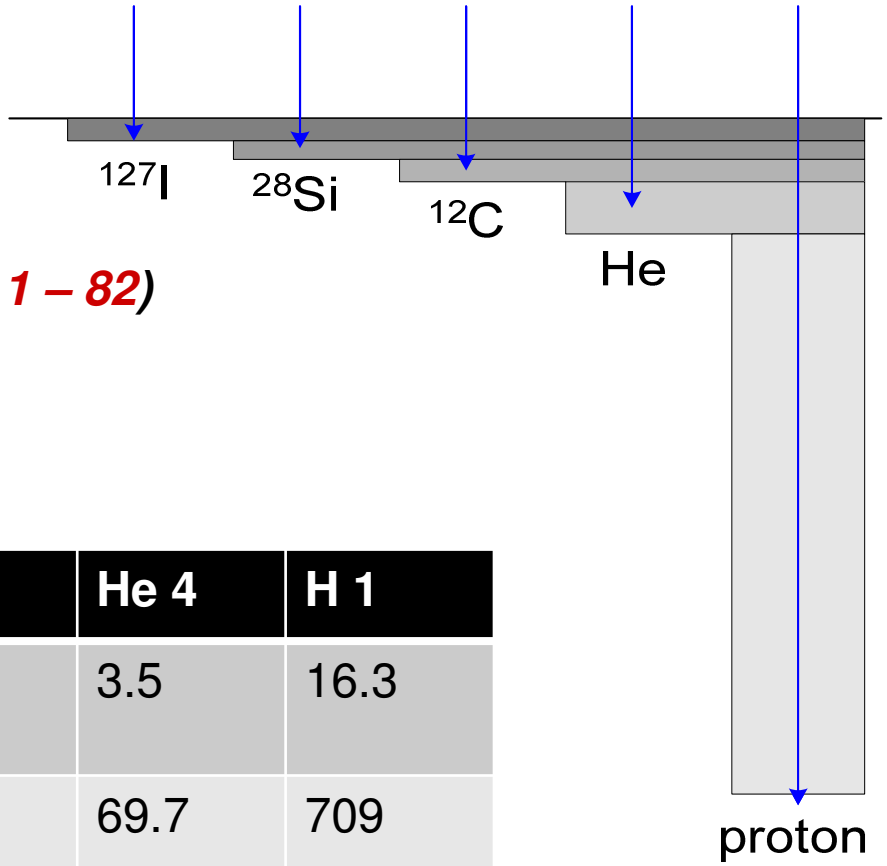

Silicon	I 127	Si 28	C 12	He 4	H 1
Range (μm) E=1 MeV	0.37	1.13	1.6	3.5	16.3
Range (μm) E=10 MeV	3.7	4.8	9.5	69.7	709

Non-Ionizing Energy Loss in Si

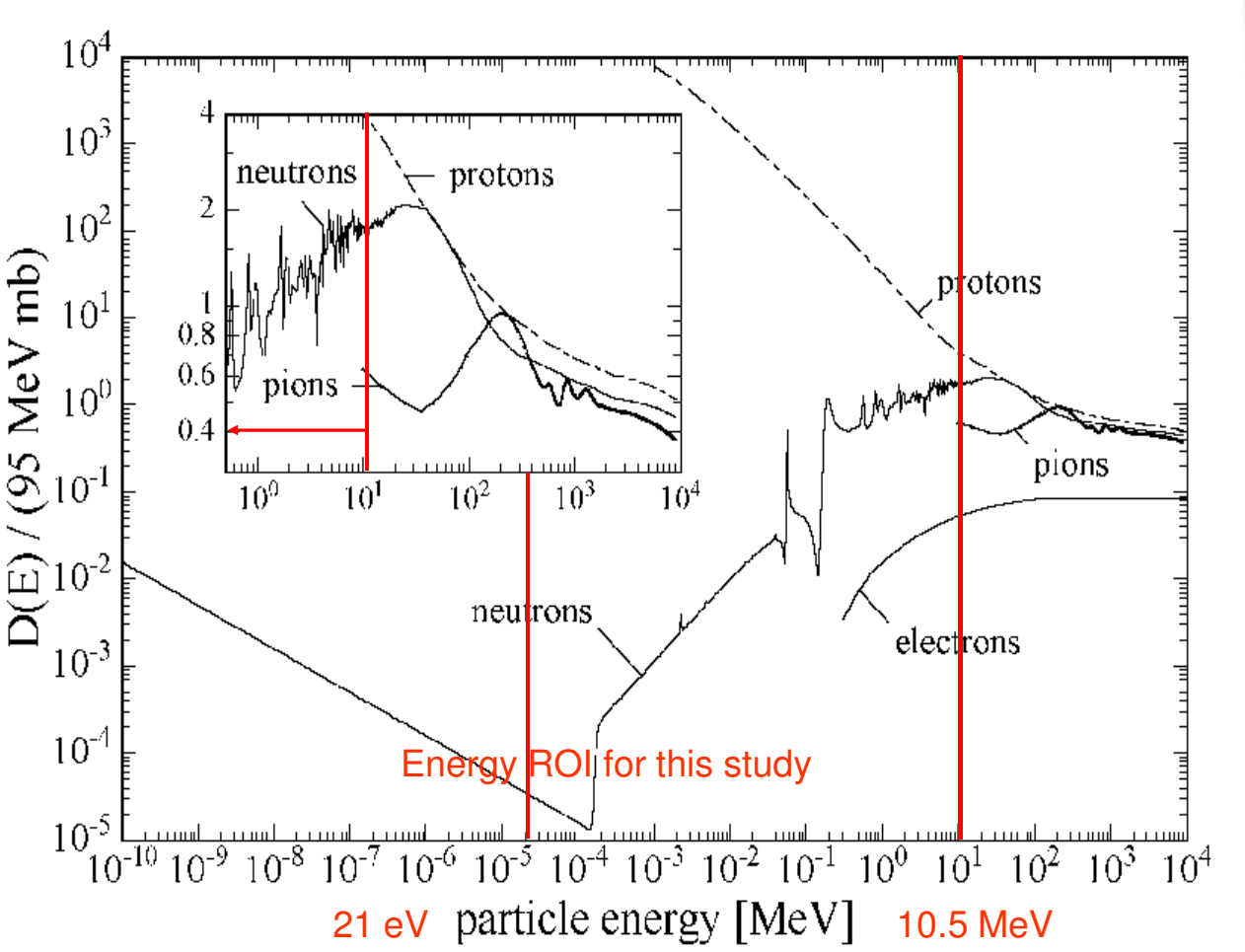

Can microprobe irradiation using (heavy) ions offer COST EFFECTIVE simulation of radiation damage produced in NOVEL semiconductor devices detectors by HIGH ENERGY p, n, e, …? (low level damage, deteriorated performance)

Single ion implantation/irradiation – point defects in single crystal semiconductors

Ion-projectile in solid

low ← **velocity** → **high**

Displace atoms
i.e. create vacancies
(nuclear stop.)

Ionize atoms
(electronic stop.)

Primary damage = Vacancy & interstitial pair

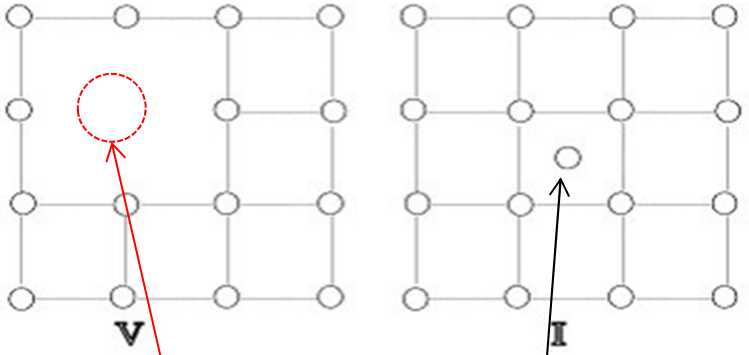

T_d =21 eV

Displaced Si atom

Interstitial Si atom

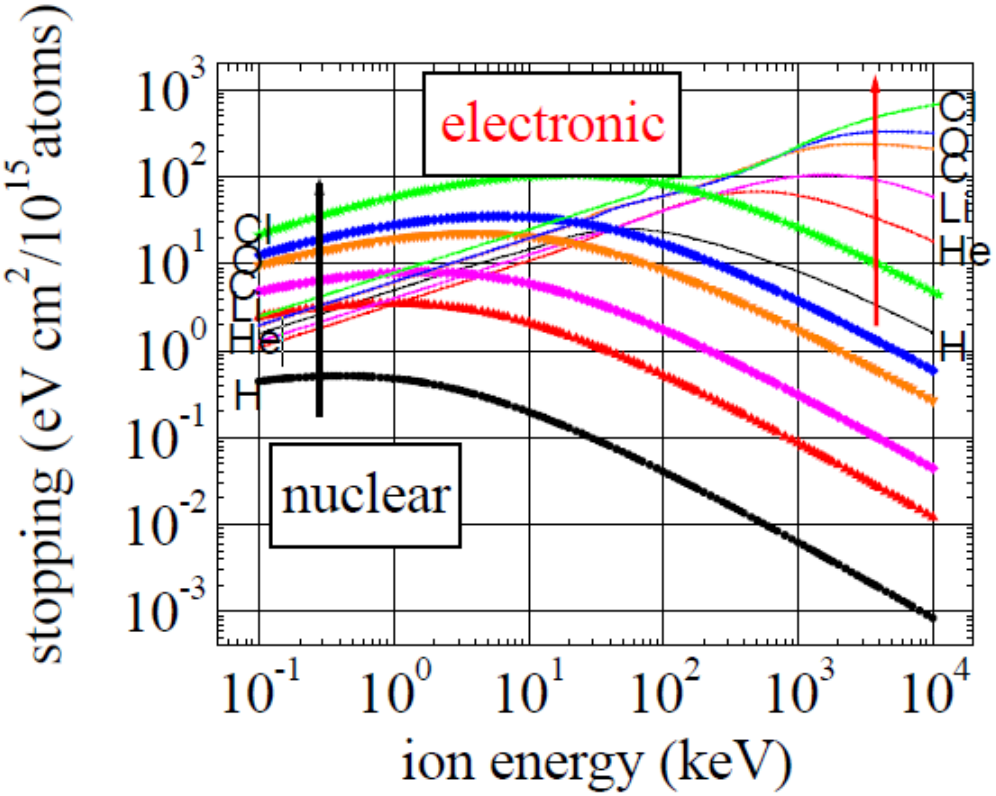

Calculated values for energy stopping of H, He, Li, C, O & Cl ions in silicon in the 100eV – 10 MeV energy range using SRIM13. Symbols: nuclear stopping; lines: electron stopping.

Cumulative primary damage distribution

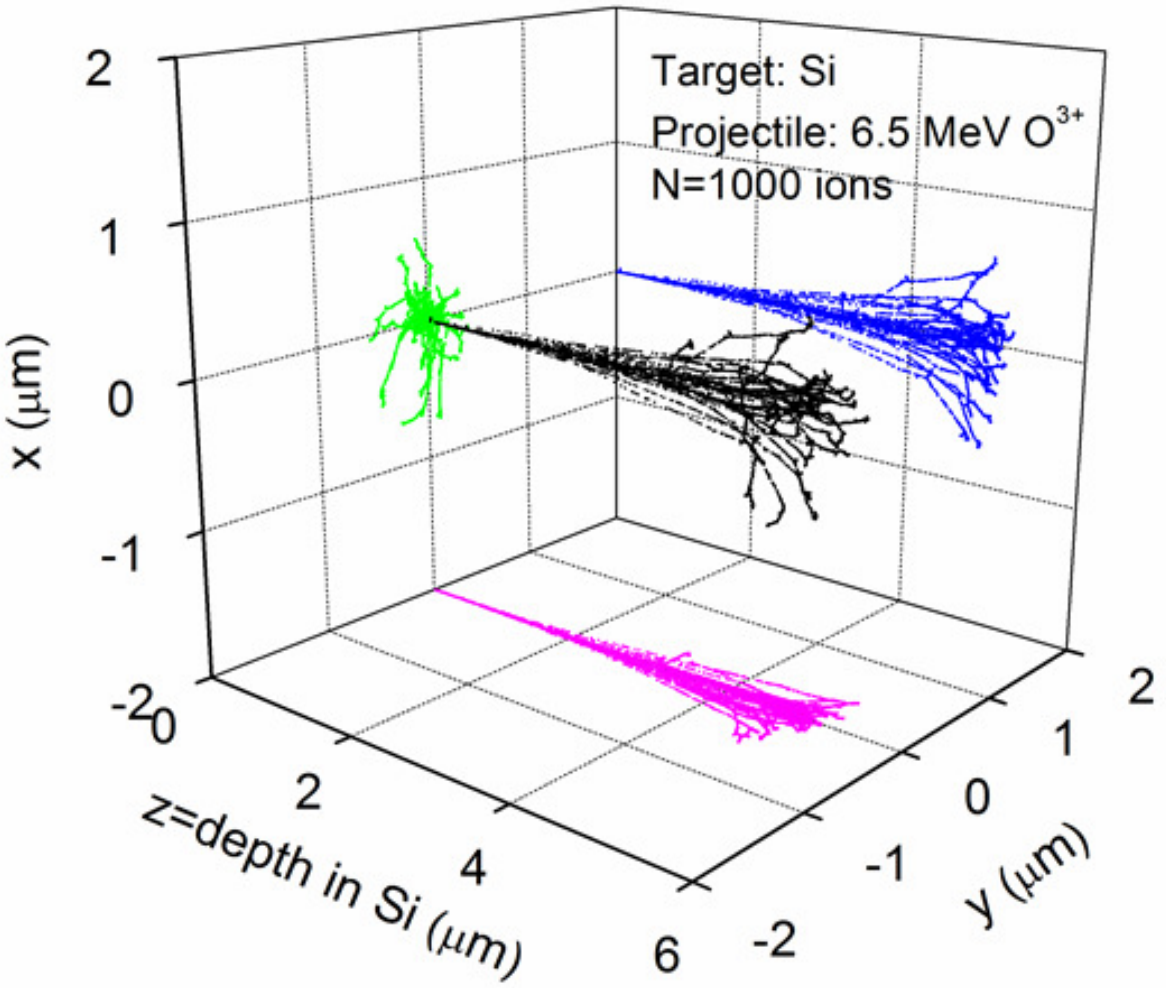

Cumulative vacancy spatial distribution (3D) (black) after implantation of 1000 oxygen ions with the same impact point (x=y=0) using the SRIM13 code; each point corresponds to one vacancy. Corresponding projections are shown in colours.

Ion implantation in "*single-ion regime*"

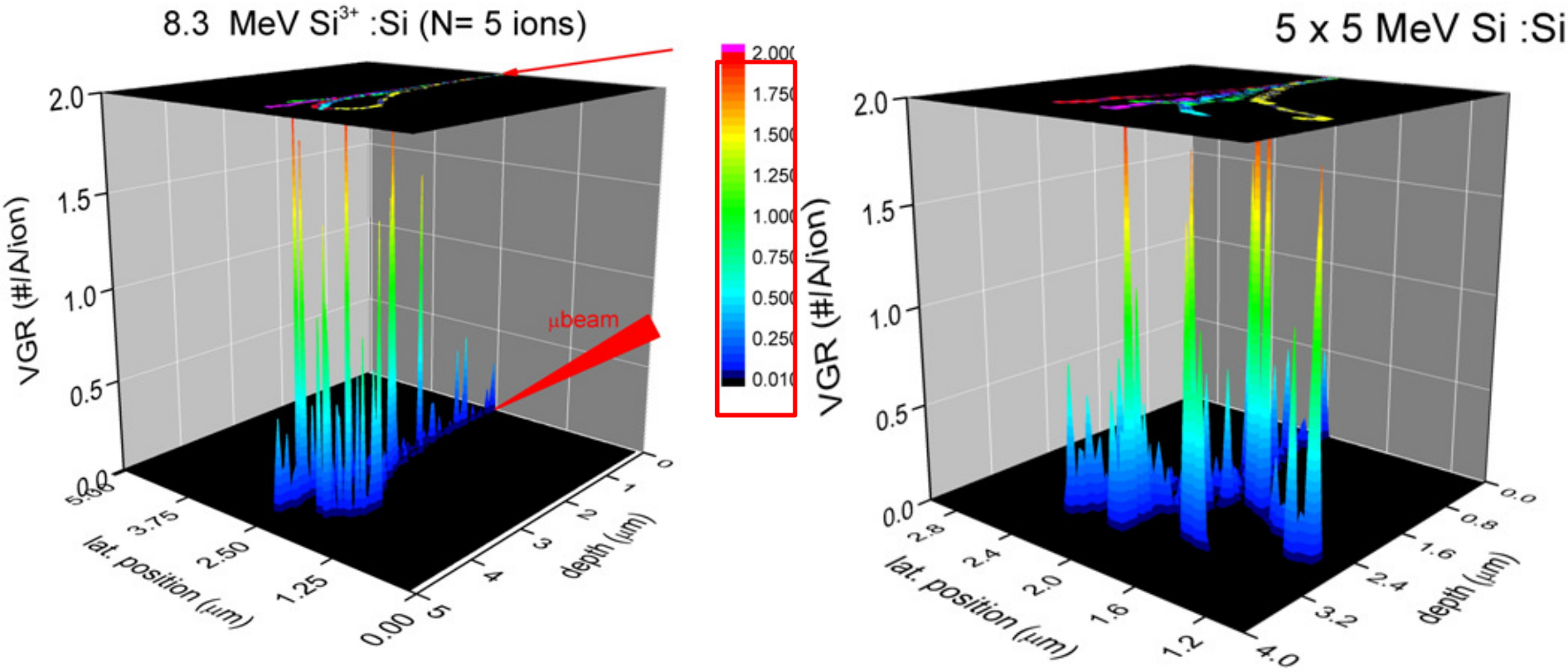

- **Projections of a vacancy yield (vacancy generation rate - VGR) on the horizontal beam plane**
- **Discrete high yield corresponding to recoil cascades**

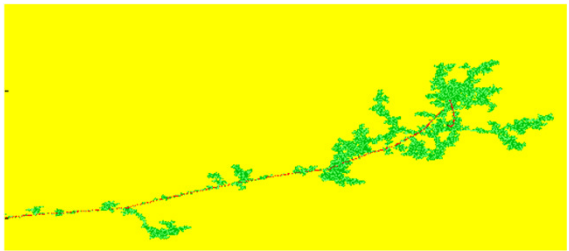

Single ion collision cascades in SiC (SRIM)

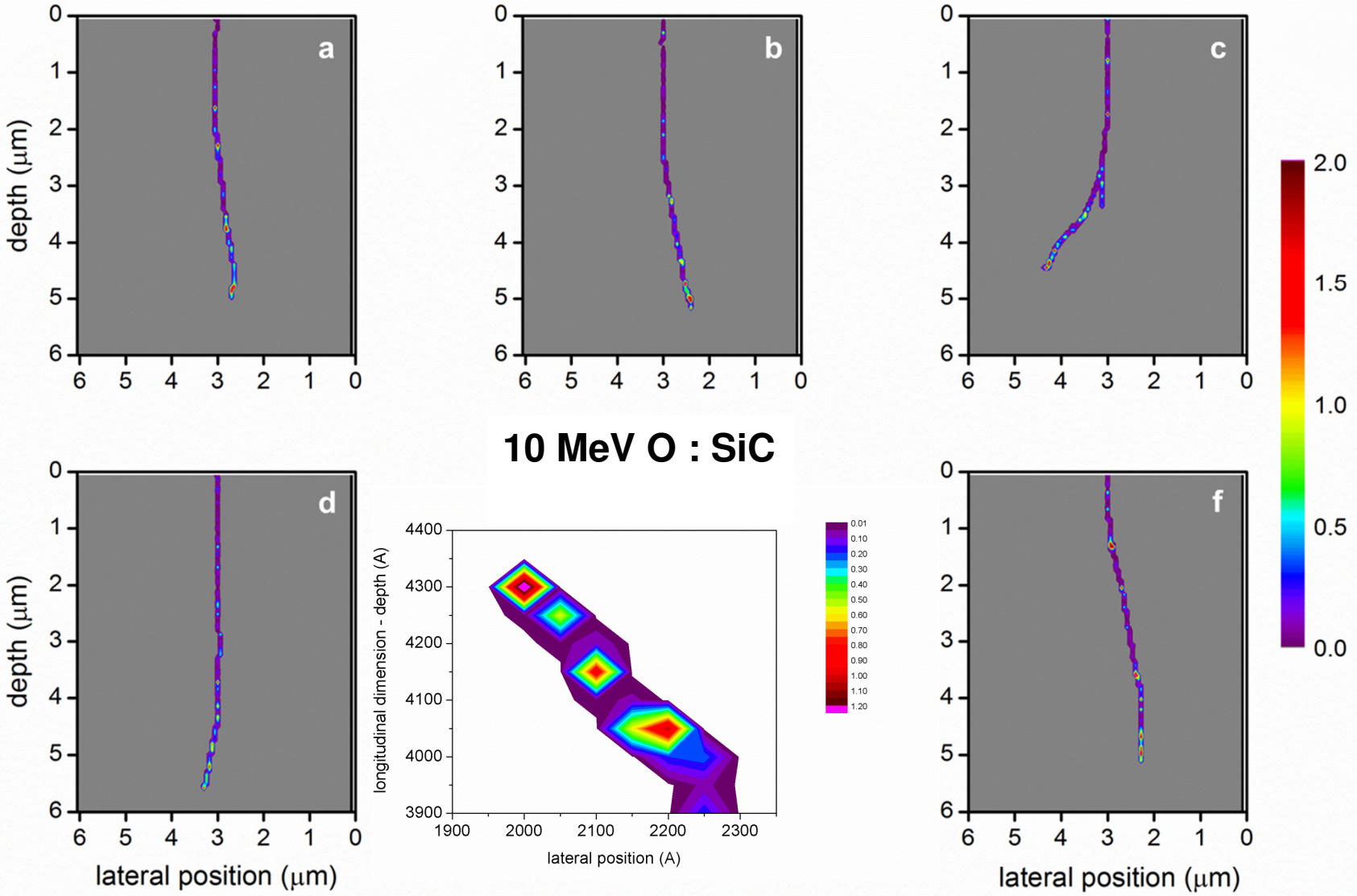

2D contour plots of the vacancy generation rate (yield) projected in 2D plane horizontal to optical beam axis.

Basic assumptions of "*single-ion*" implantation

- **The thermally stimulated recovery or reorganization of final defects as a result of additional radiation annealing from demonstrated weakly overlapping cascades is reasonable to be assumed negligible.**

- **The final defect species which are formed from primary defects generated in locally disordered regions along ion cascades can be considered a result of the single ion hit.**

Secondary point defects in single crystal SC

Missing atoms from hexagonal crystal lattice

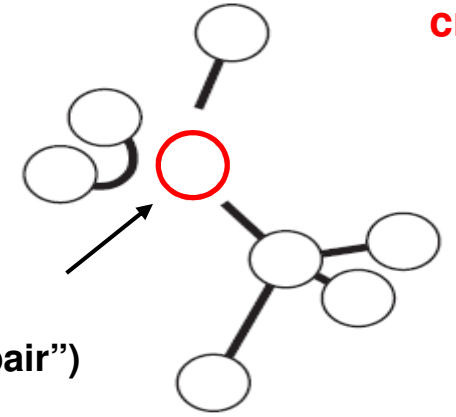

Single vacancy

-highly mobile at RT
→ easy to recombine (“repair”)

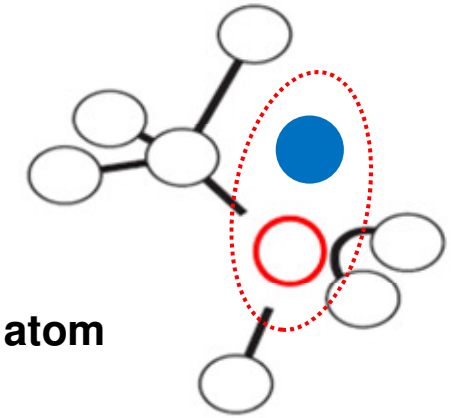

Vacancy & Interstitial atom

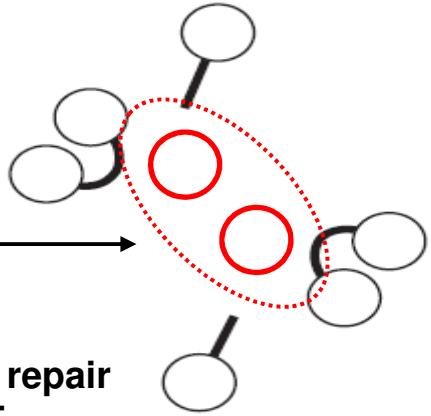

Double vacancy or divacancy

-”double trouble”→hard to repair
→ stable point defect at RT
→ trap free charge in SC, etc…

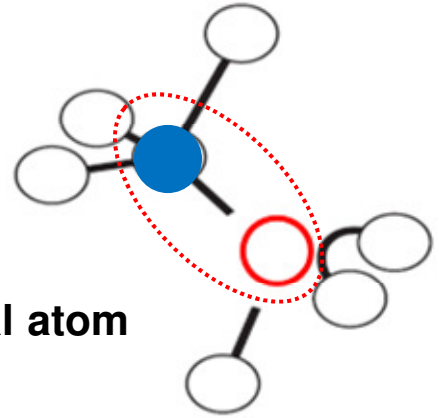

Vacancy & Substitutional atom

-donors

Point defects in n-Si

I. Capan et. al., J. Phys.: Condens. Matter 17 (2005) S2229

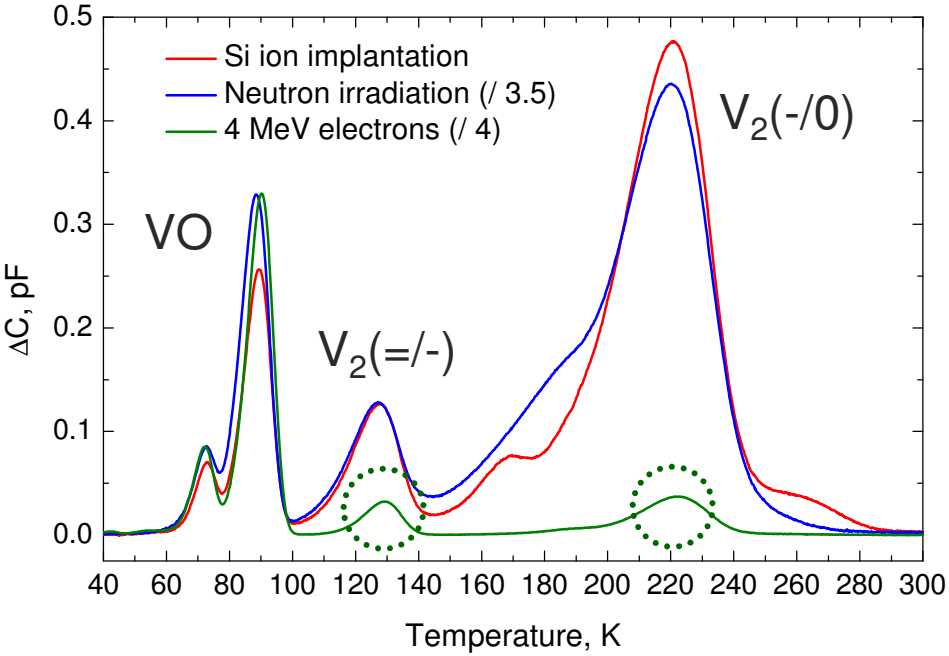

DLTS spectra of n-CZ-Si after irradiation with different types of ionizing radiation.

L. Vines et al., PHYSICAL REVIEW B **79**, 075206 (2009)

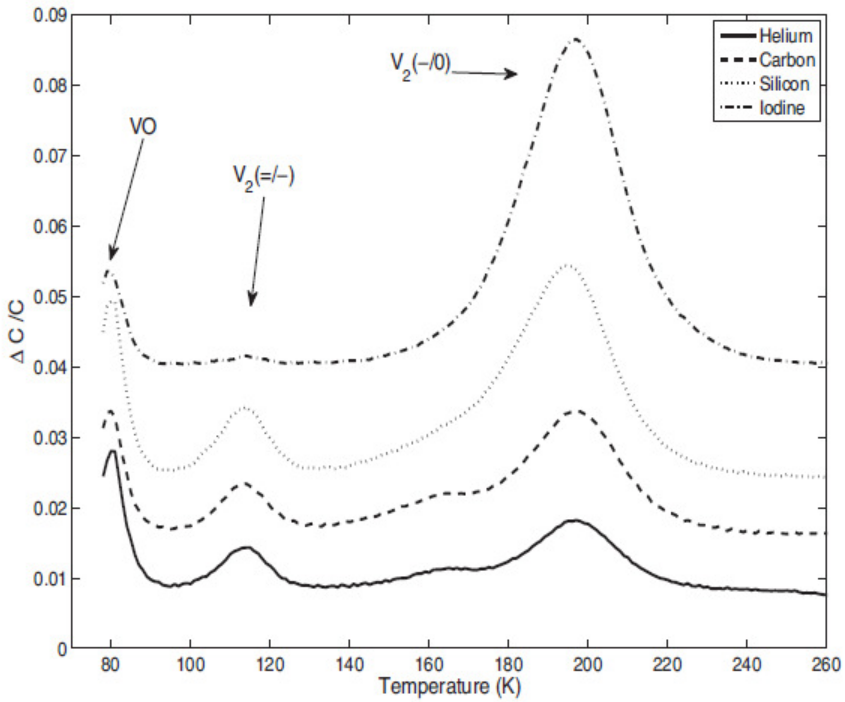

FIG. 2. DLTS spectra of epi-Si after implantation with different ions. Offsets have been applied to separate the lines for clarity. $\Delta C/C$ is the DLTS signal (ΔC) divided by the reverse bias capacitance (C).

Radiation detection by pristine device

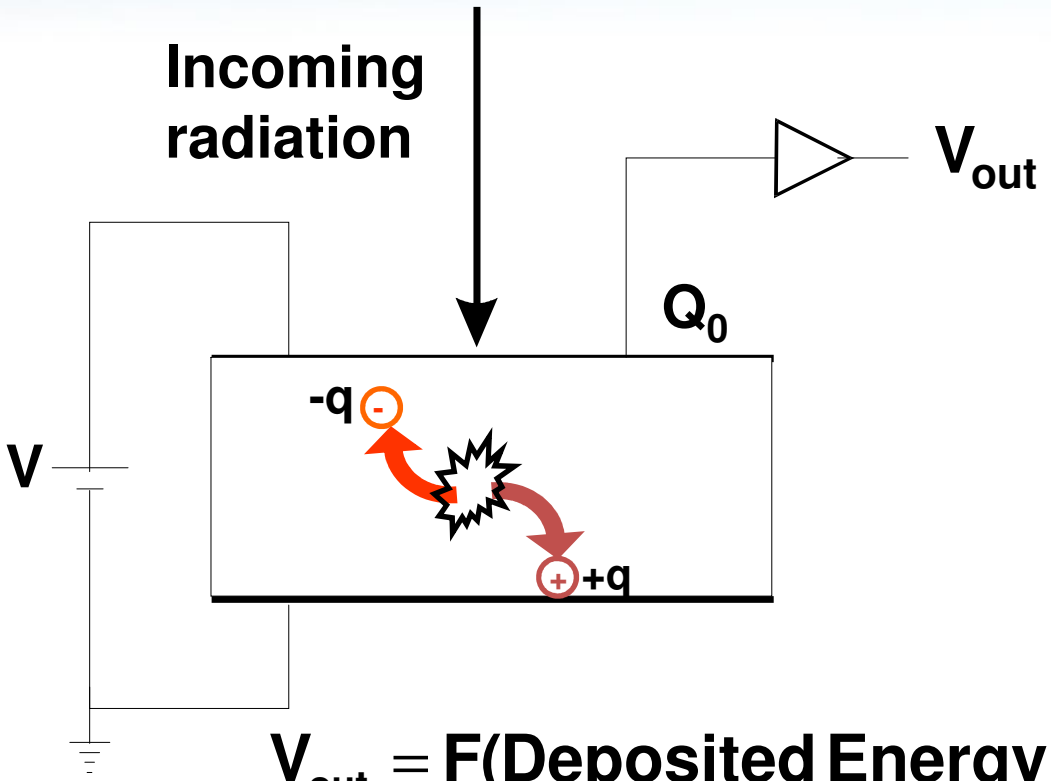

Deposited Energy

Moving charge q

Induced charge Q_0

Output Signal V_{out}

$$V_{out} = F(\text{Deposited Energy}, \text{Free Carrier Transport})$$

Nuclear spectroscopy

Material characterisation

Ion Beam Induced Charge (IBIC) Microscopy

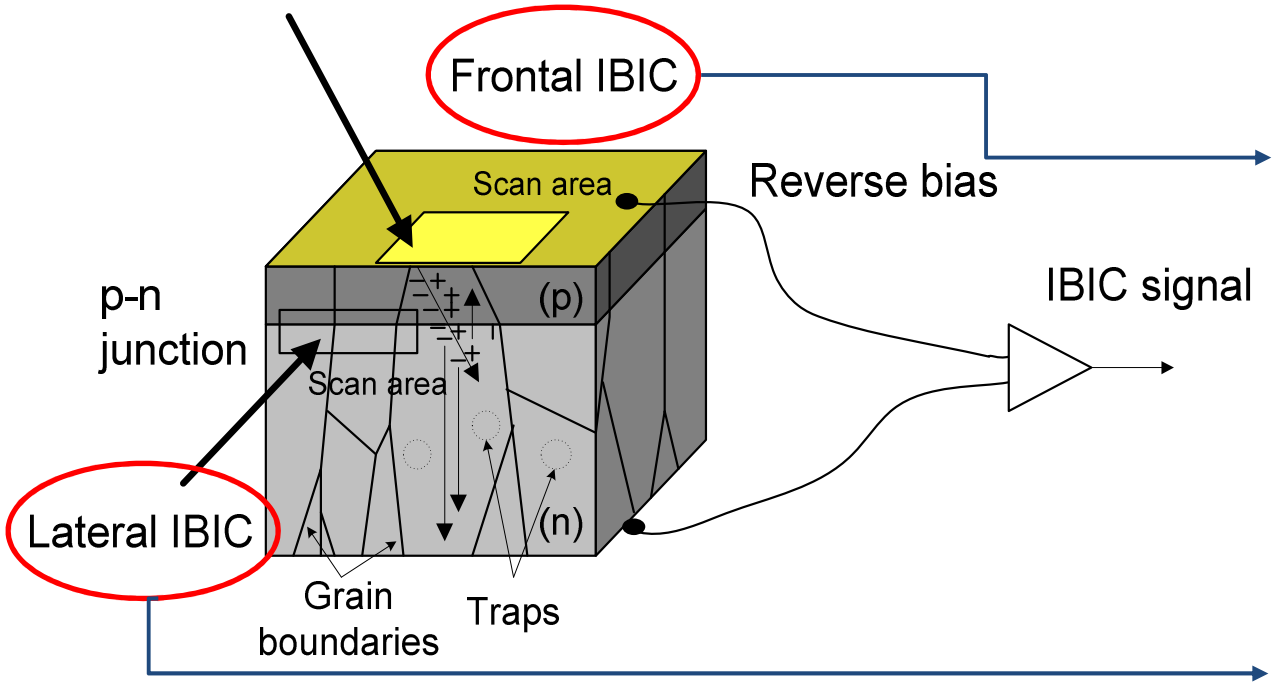

CVD diamond (1997)

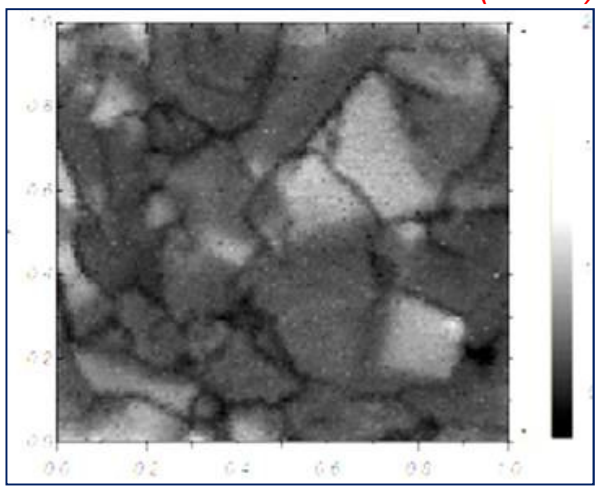

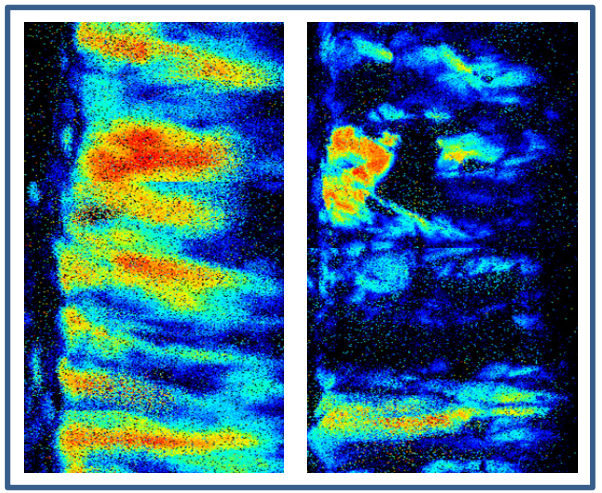

IBIC **-** *single ion technique for imaging of microscopic distribution of charge transport properties related to CCE!*
- Imaging of grain boundaries, defects, electric field etc.

Two regimes of damage studies in materials:

I. *Low level of radiation damage (eg. particle detection, microdosimetry, electronics)*

- ✓ Linear behaviour of degradation of the CCE vs. ion fluence
- ✓ Damage does not influence the electrical / structural properties of the material
- ✓ Electronic trap density proportional to vacancy density
- ✓ Shockley-Read-Hall model

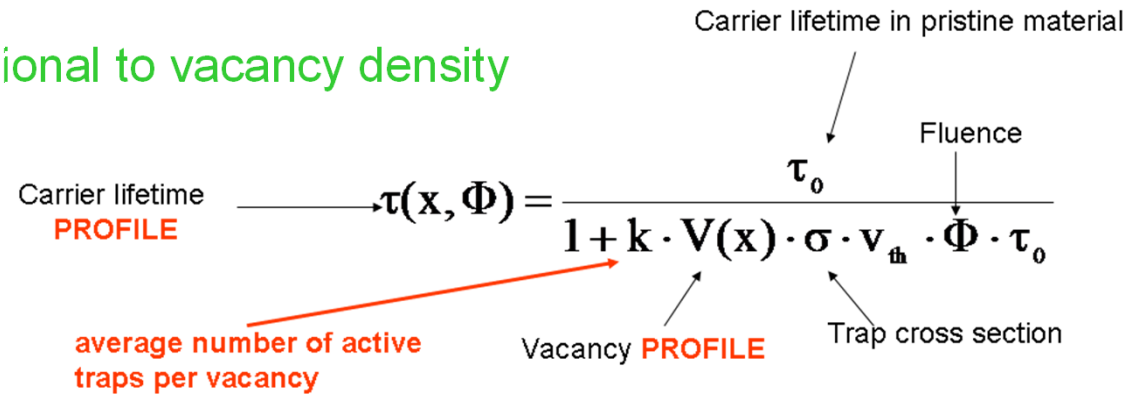

II. *High level of damage (IBMM for advanced material technologies and device fabrication)*

1. Non linear behaviour of degradation of the charge collection efficiency vs. ion fluence
2. Damage influences the electrical/structural properties of the material

Radiation detection by LIGHT damaged semiconductor detector

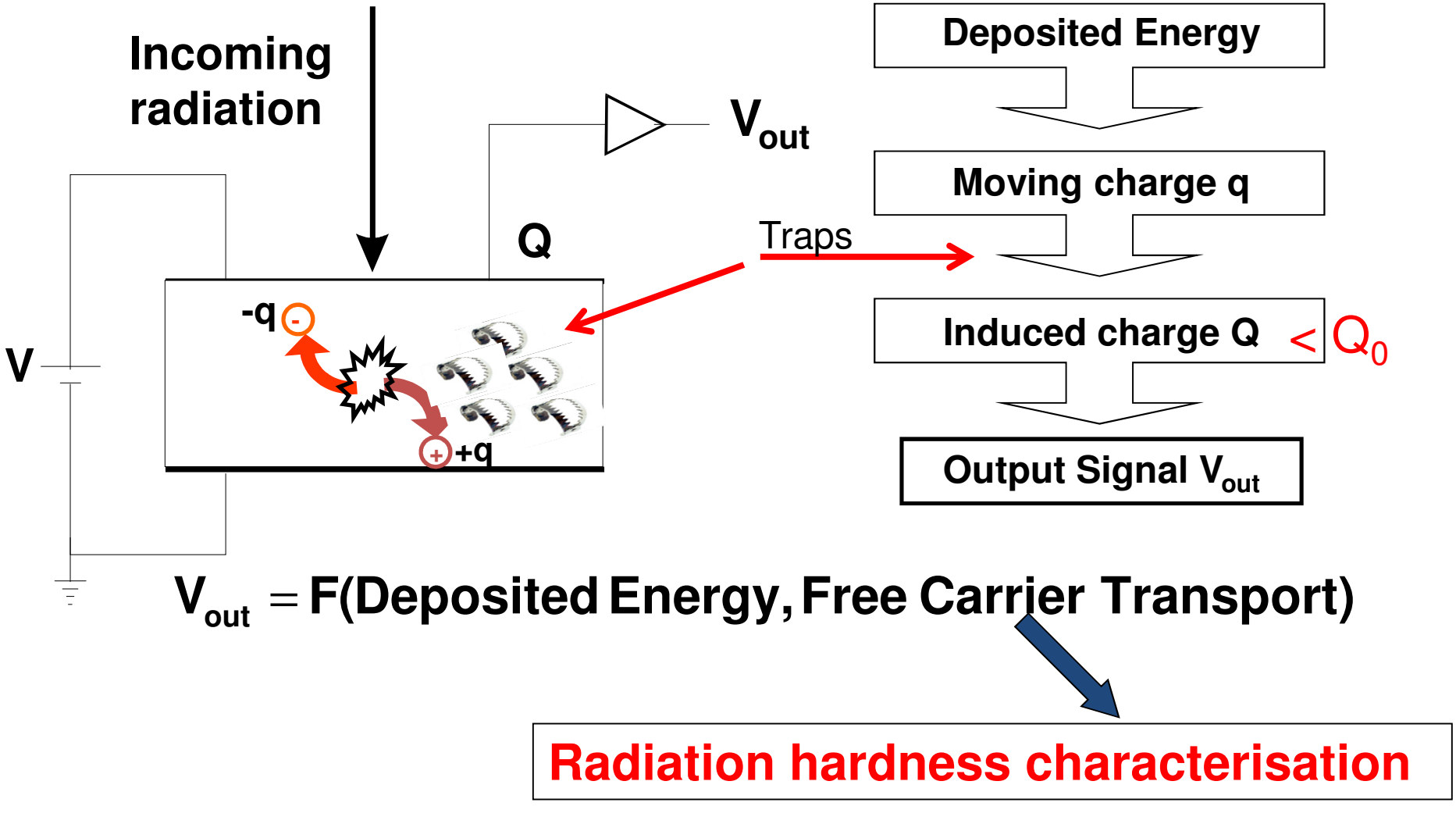

Quantization of radiation damage by Non Ionizing Energy Loss (NIEL) theory

Radiation damage function
(RD42 Collaboration)

$$\alpha = \frac{\Delta I}{V \cdot \Phi_{eq}}$$

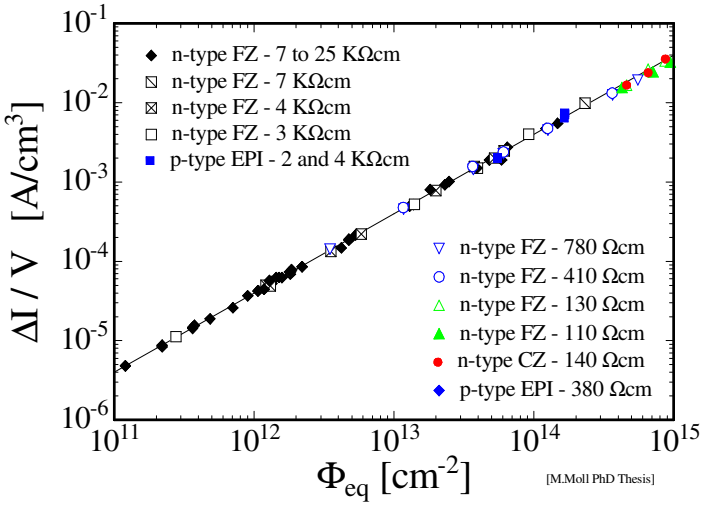

Damage correlation by Non-Ionizing Energy Loss (NIEL)
(G.P. Summers et.al., IEEE Trans. Nucl. Sci., vol.40 (1993) 1372)

$$\alpha \cdot \Phi_{eq} \Leftrightarrow K_{ed} \cdot D_d \qquad D_d = \langle NIEL \rangle \cdot \Phi$$

How to calculate NIEL for ions (analytical approach)
(S.R.Messenger et.al, IEEE Trans. Nucl. Sci., vol. 46 (6) (1999) 1595)

$$\langle NIEL \rangle = T_d \cdot \langle V(x) \rangle \cdot \frac{1}{\rho}$$

$$\frac{Q_0}{Q} = 1 + K_{ed} \cdot \Phi \cdot \langle NIEL \rangle$$

$D_d = 10^{10} - 10^{13}$ MeV/g

K_{ed} – equivalent damage factor (g/MeV)
property of material? and?

Φ – ionizing radiation fluence (cm^{-2})

$\langle NIEL \rangle$ – average energy of corr. ionizing radiation used for displacement of lattice atoms ($MeVcm^2g^{-1}$)

D_d – displacement damage dose ($MeVg^{-1}$)

Protocol suitable for studies

(12th ICNMTA2010)

Pastuovic, Jaksic, Kalinka, Novak, Simon, IEEE Trans. Nucl. Sci. 56 (2009) 2457

SC device, e.g. diode

2D distribution of the IBIC signal amplitude obtained in frontal measurement mode on a pristine diode

ZOOM in view of the selected area for a focused He ion beam irradiation

2D distribution of the IBIC signal amplitude obtained with a selected *probe*

IBIC spectra obtained form whole irradiated area

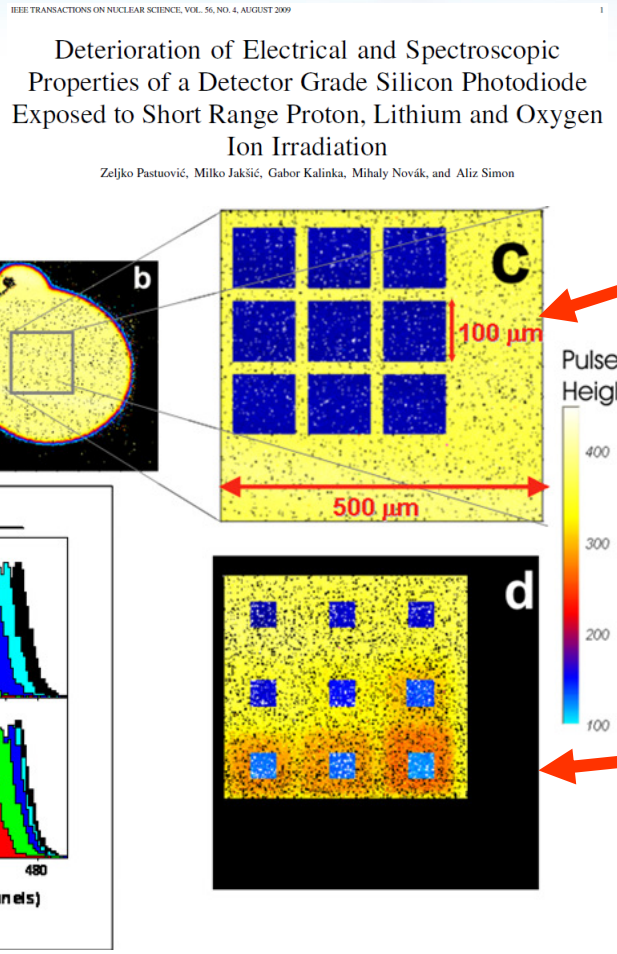

Adv.: single IBIC measurement for one probe–damage system → minimising costs

Ion detection by partly damaged *n* - FZ Si diodes

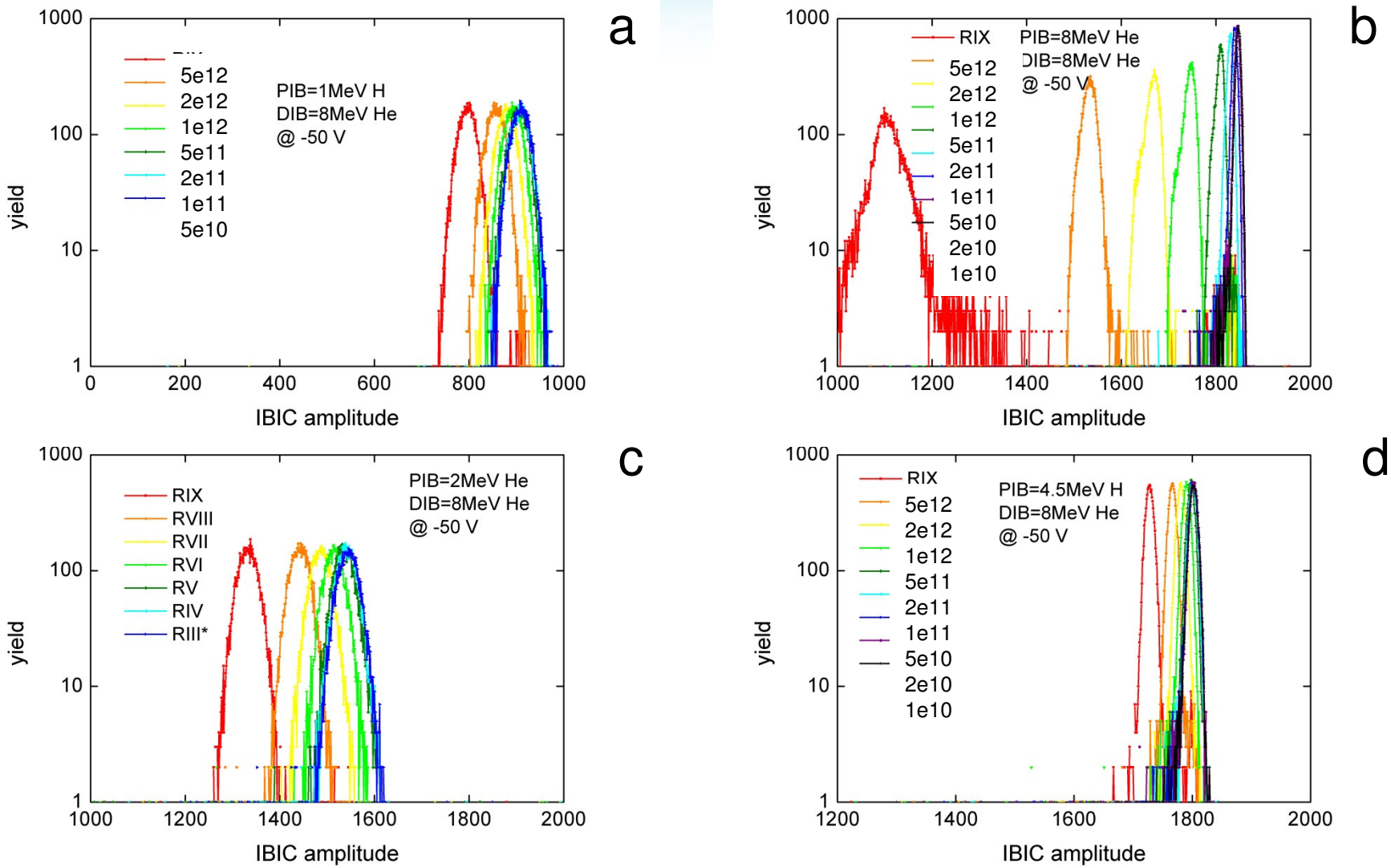

IBIC spectra obtained for detection of (a) 1 MeV H, (b) 8 MeV He, (c) 2 MeV He and (d) 4.5 MeV H ions (PIB) using the same partly damaged FZ Si diode pattern irradiated with 8 MeV He ion up in the 1e10 – 5e12 cm-2 fluence range.

Model to interpret IBIC data

(13th ICNMTA2012)

$$CCE(\Phi) \equiv 1 - K_e^* \cdot \Phi_e^*$$

- ✓ **Full depletion regime**
- ✓ **Hole contribution negligible**
- ✓ **Saturation drift velocity**
- ✓ **Semi-analytical expression**

APPLIED PHYSICS LETTERS 98, 092101 (2011)

Probability of divacancy trap production in silicon diodes exposed to focused ion beam irradiation

Željko Pastuović,[1,a)] Ettore Vittone,[2] Ivana Capan,[1] and Milko Jakšić[1]
[1]*Department for Experimental Physics, Ruđer Bošković Institute, P.O. Box 180, 10002 Zagreb, Croatia*
[2]*Department of Experimental Physics, NIS Excellence Centre, University of Torino, via P. Giuria 1, 10250 Torino, Italy*

(Received 17 December 2010; accepted 2 February 2011; published online 28 February 2011)

Ion probe energy loss

Vacancy profile

Weighting potential

$$\Phi^* = \text{Effective Fluence} = \Phi \cdot \left\{ \int_0^w dz \cdot \left[\tilde{E}_{Ion}(z) \cdot Vac(z) \cdot \left(1 - \frac{z}{w} \right) \right] \right\}$$

$$K_e^* = \text{effective damage factor} = k_e \cdot \sigma_e \cdot \frac{v_{th}}{\langle v_e \rangle}$$

Average carrier drift velocity

Average number of active trap per vacancy (IBIC)

Capture cross section of traps generated by ions (DLTS)

Better radiation hardness is characterised by LOWER $k_e \cdot \sigma_e$ or K_e^* value

Free carrier generation & motion

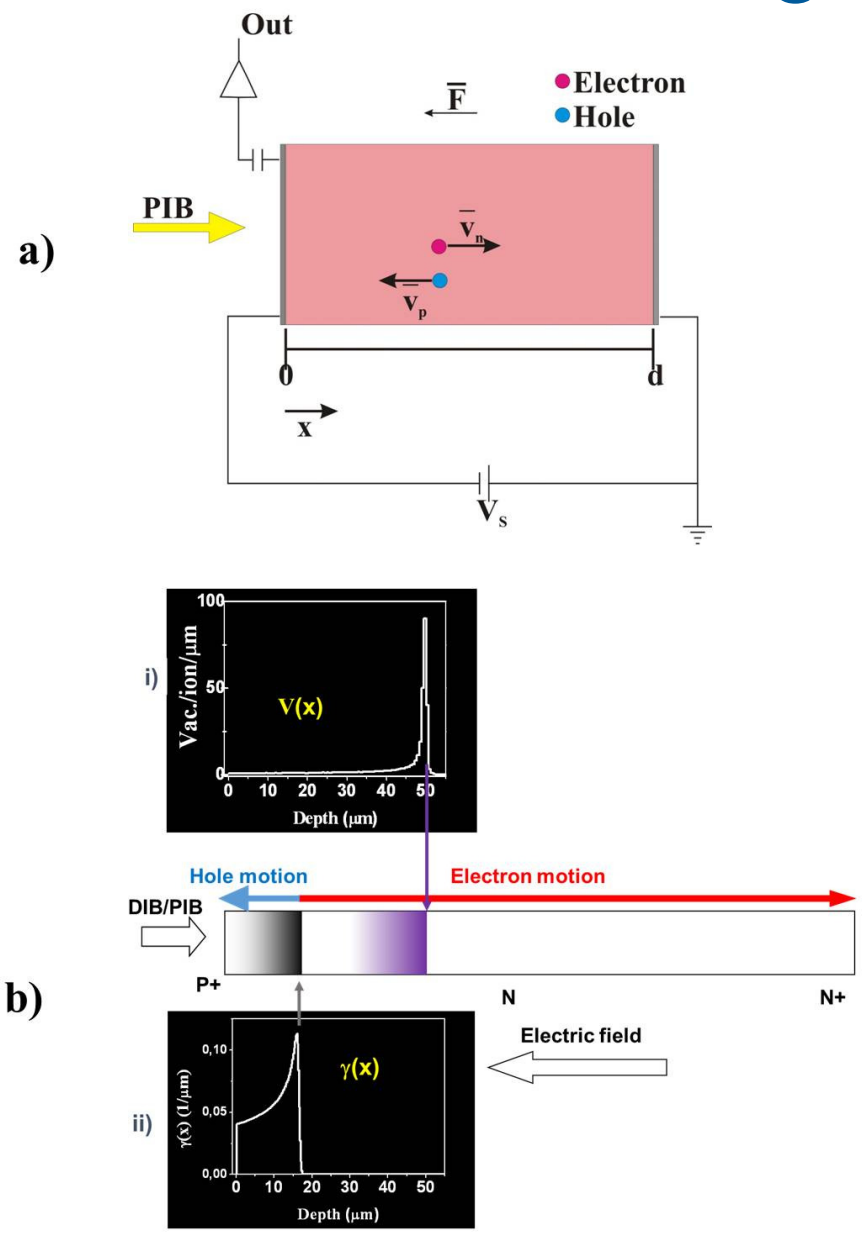

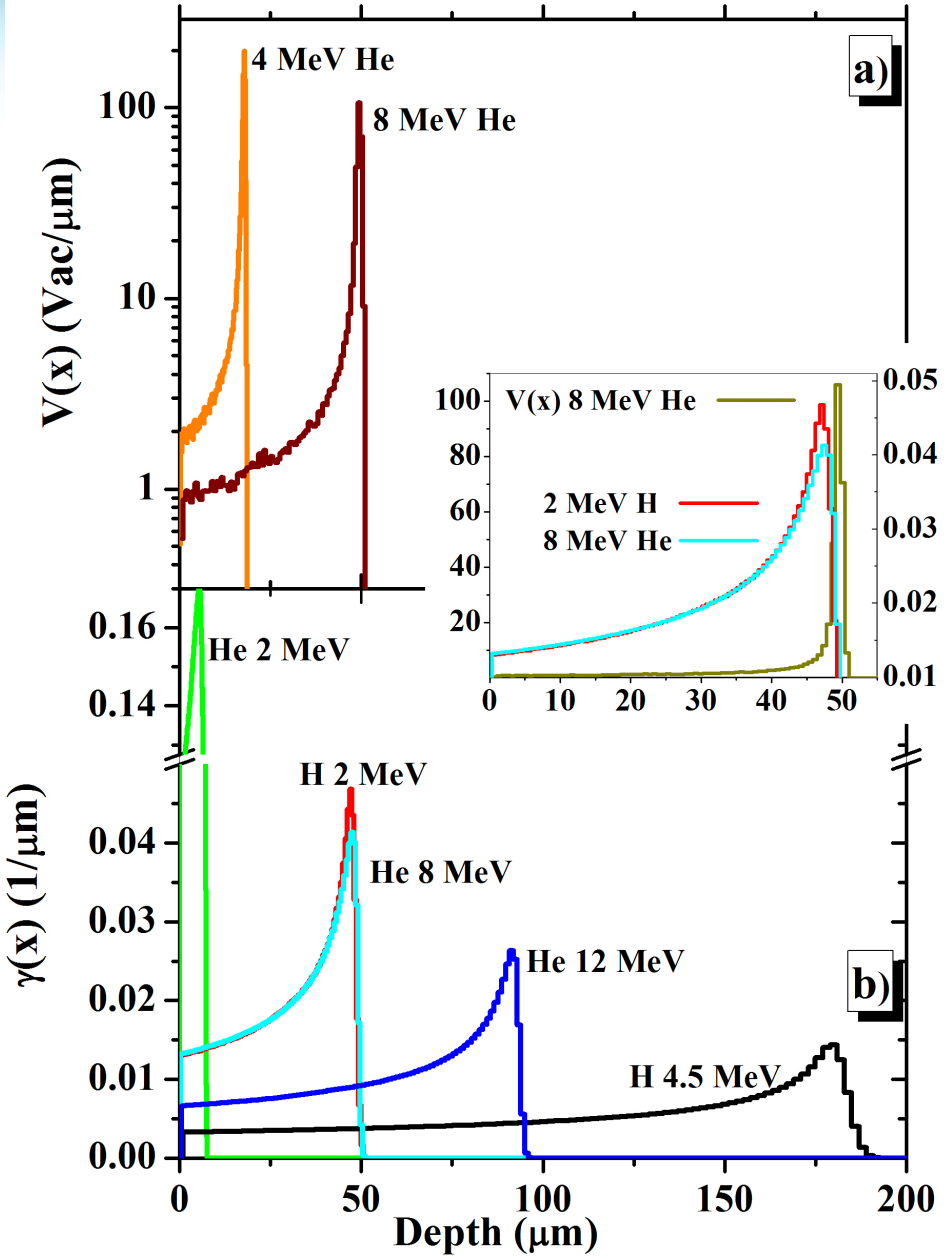

Condensation of CCE data

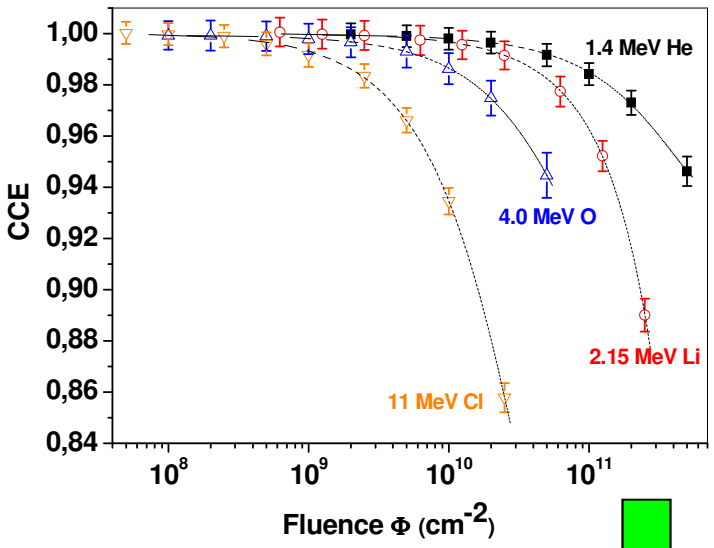

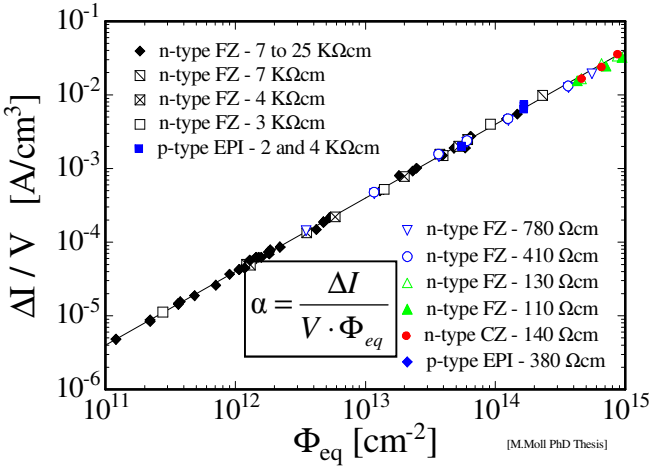

$$K^* = \frac{k_e \cdot \sigma_e \cdot v_{th}}{v_e} = (1.09 \pm 0.02) \cdot 10^{-15}\ \mathrm{cm}^2$$

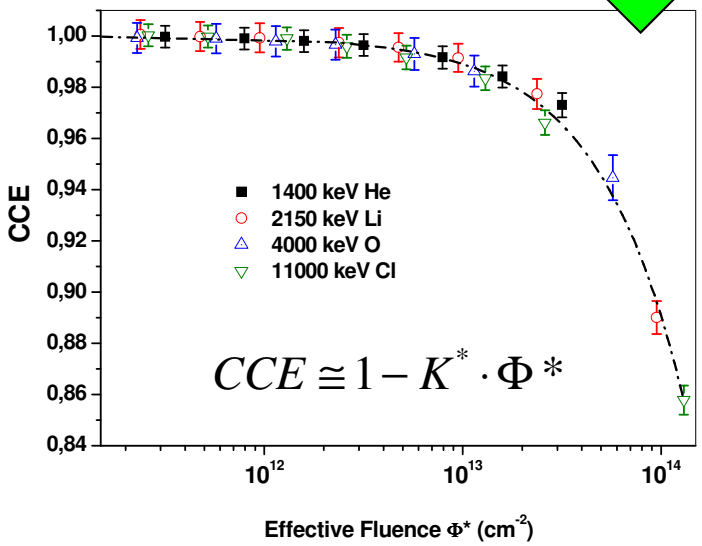

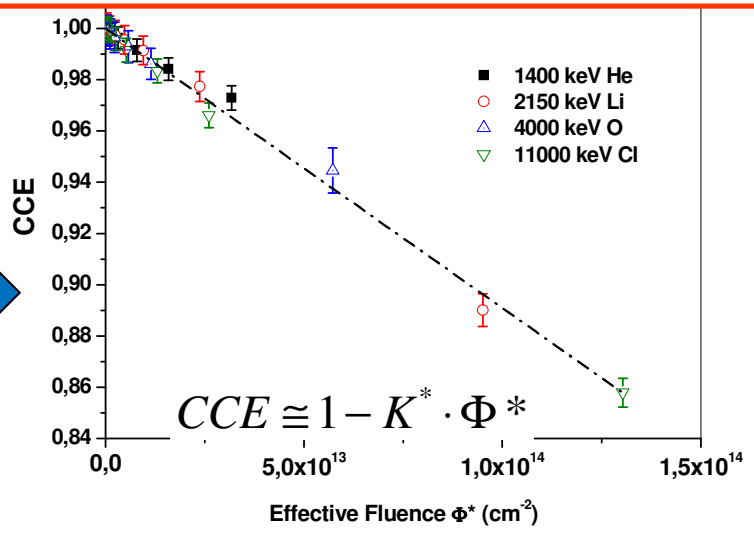

Light ion detection using partly damaged diodes

CHARGE COLLECTION EFFICIENCY PROFILES

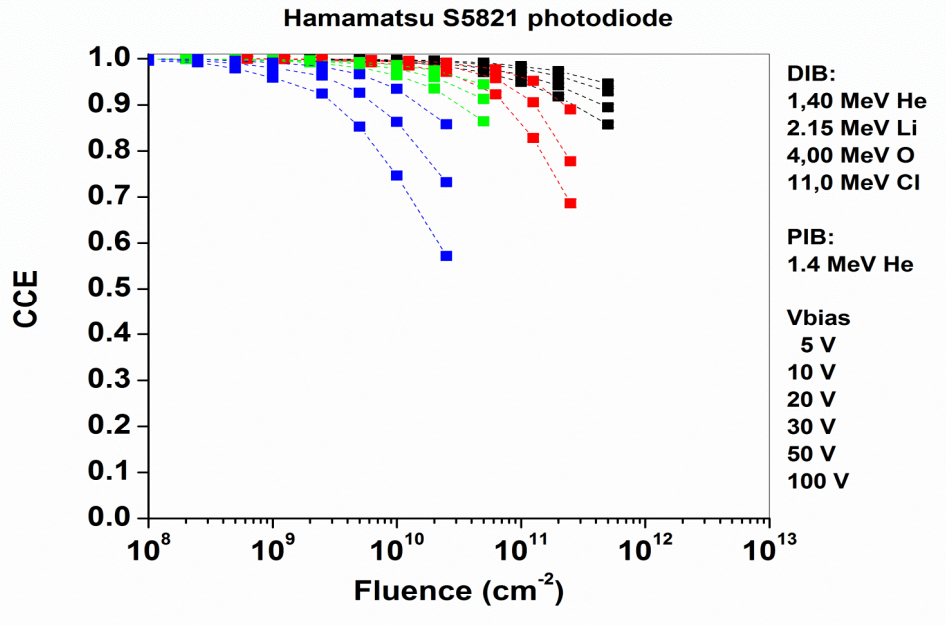

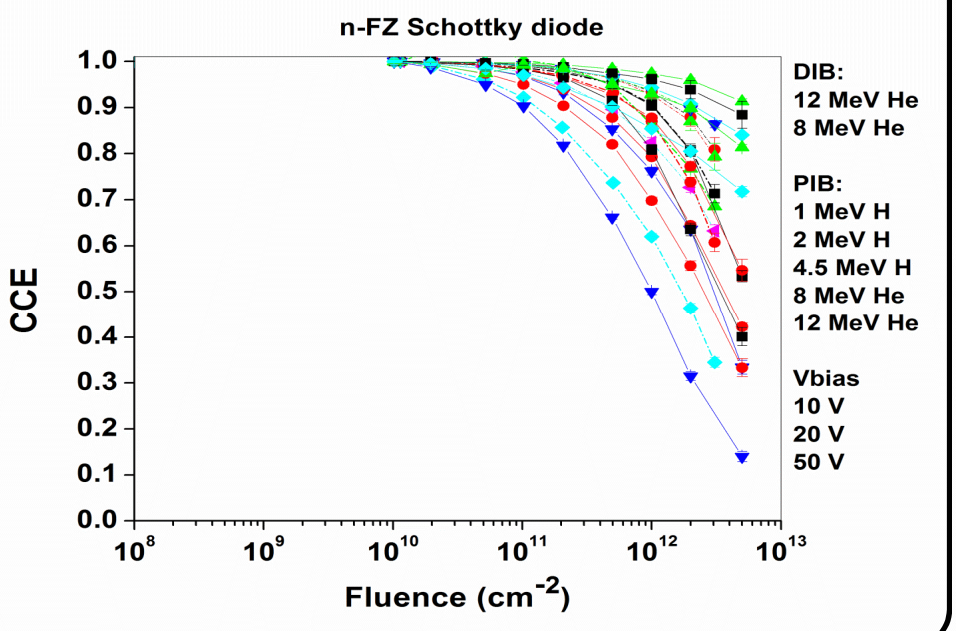

PROBLEM: Radiation damage effects incl. CCE degradation in SC devices depend on :
1) FLUENCE, 2) ION - DAMAGING PARTICLE (DIB), 3) BIAS - POLARIZATION STATE,
4) PROBE - DETECTED PARTICLE (PIB), and 5) TYPE OF MATERIAL.

Validation of extended model

(15th ICNMTA2016)

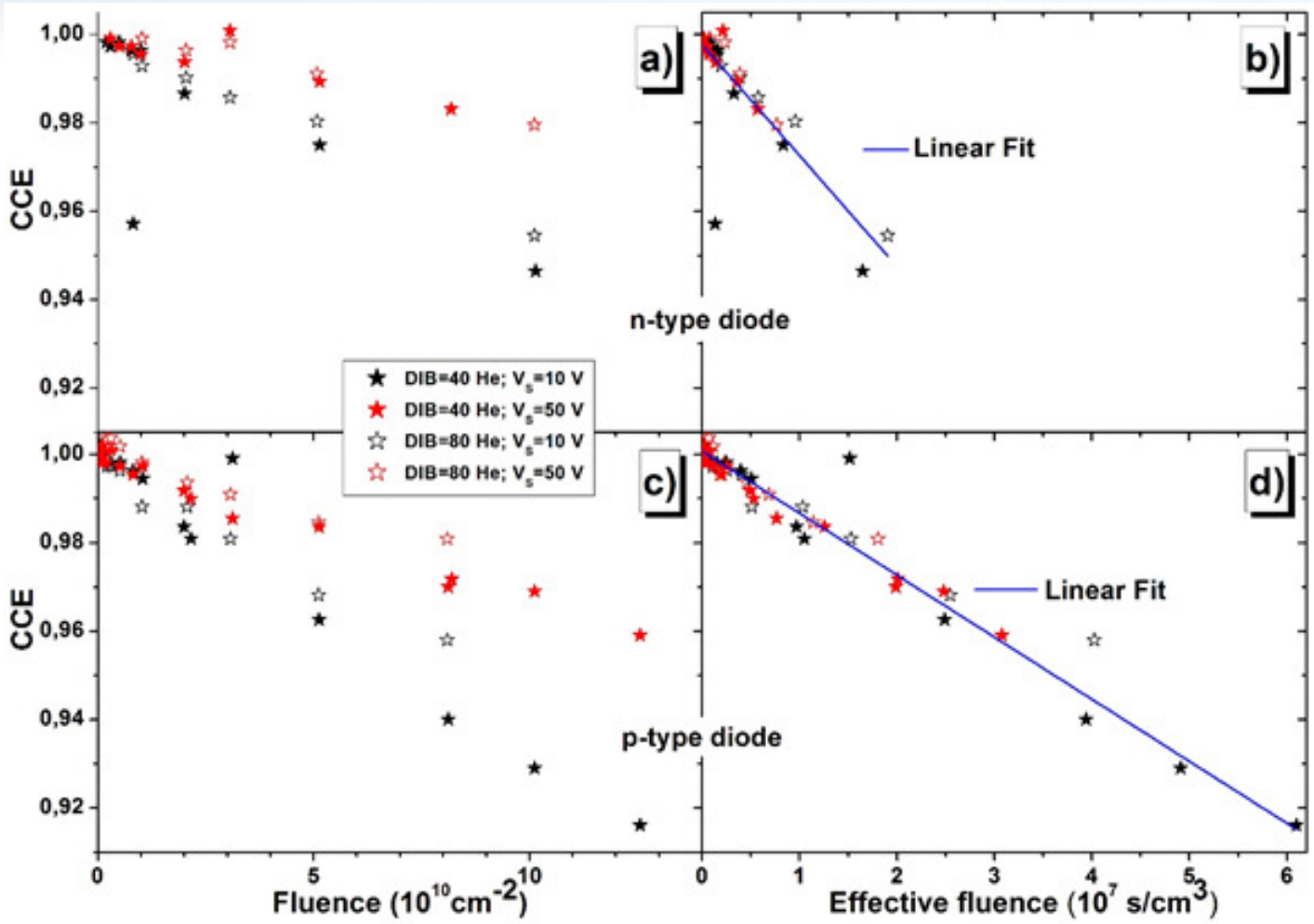

Linearization of the CCE degradation distributions for various PIB, DIB and bias settings using the extended model* for simulation of experimental values (symbols).

Nuclear Instruments and Methods in Physics Research Section B: Beam Interactions with Materials and Atoms

Volume 372, 1 April 2016, Pages 128–142

Charge collection efficiency degradation induced by MeV ions in semiconductor devices: Model and experiment

E. Vittone[a], Z. Pastuovic[b], M.B.H. Breese[c], J. Garcia Lopez[d], M. Jaksic[e], J. Raisanen[f], R. Siegele[b], A. Simon[g,h], G. Vizkelethy[i,1]

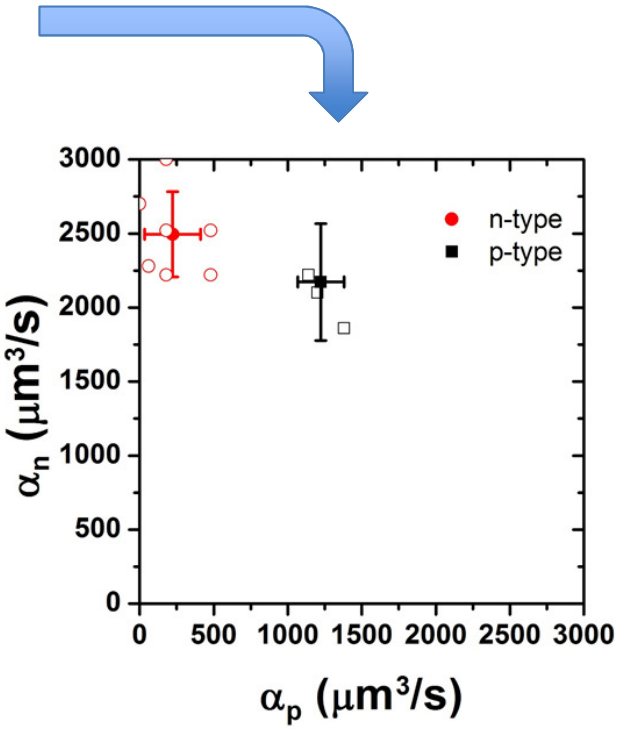

Calculated recombination factors for electron and hole trapping

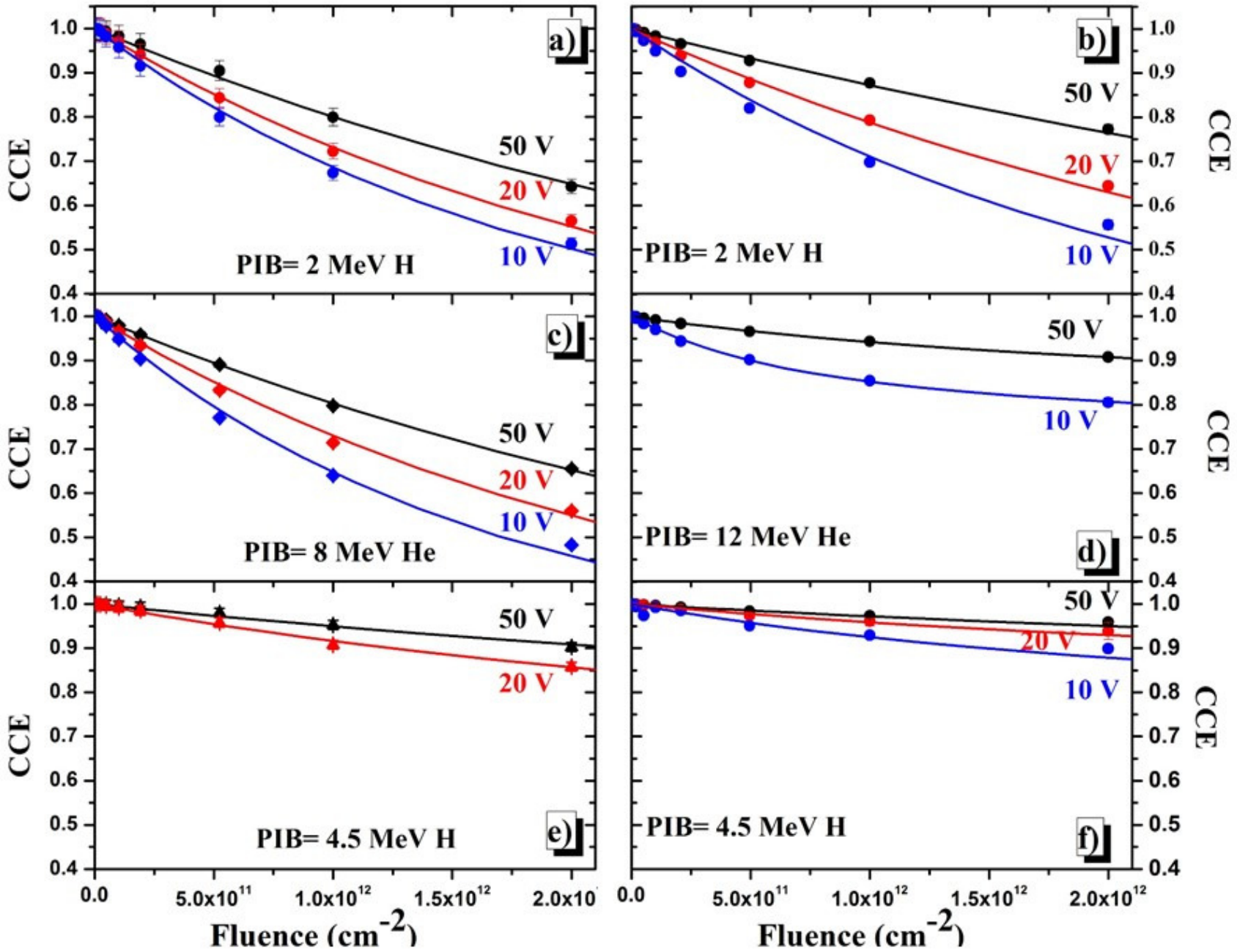
a)
b)
c)
d)
e)
f)
50 V
20 V
10 V
PIB= 2 MeV H
PIB= 8 MeV He
PIB= 12 MeV He
PIB= 4.5 MeV H
CCE
Fluence (cm^{-2})
0.0
5.0x10^{11}
1.0x10^{12}
1.5x10^{12}
2.0x10^{12}

Motivation for rad. hard. studies of SiC detectors

- Semiconductor detectors equipped with a converter like 6LiF or 10B can currently be considered a very interesting alternative to conventional neutron detectors, especially because of their compactness and reliability.
- Search for new devices which are proved to be very suitable for neutron detection, dosimetry and beam monitoring.
- Silicon carbide (SiC) radiation detectors are being developed for high-temperature applications in harsh radiation environments for over a decade.
- Capability to withstand high radiation doses on high energy protons, gammas and neutrons should largely overcome the performances of Si.
- Recent advances in epi 4H-SiC growth offers production of high-performing detectors of ionizing radiation

E-SiCure project

(NATO SPS Grant #985215)

Problem

SNM monitoring

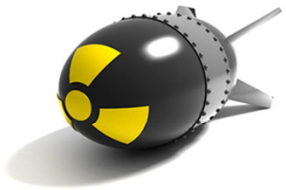

Constraint

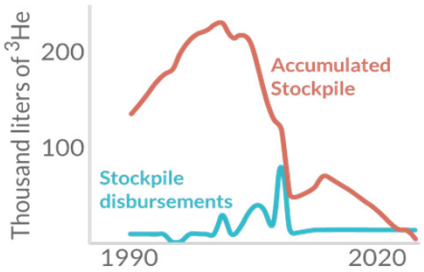

Solution

Detector

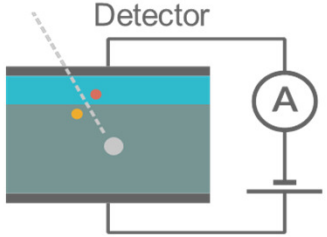

Material

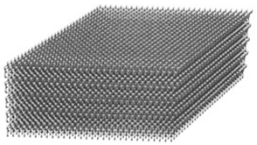

Defect

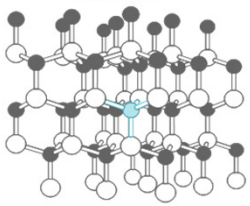

Goal

Engineering Detector-grade SiC

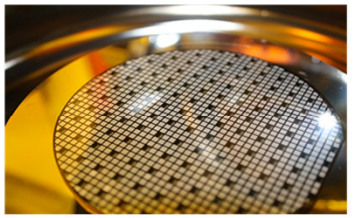

Success Criteria

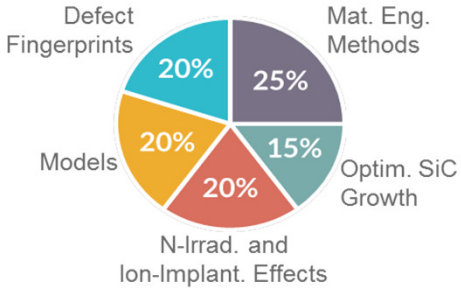

Australian Government | ansto

E-SiCure Project

Engineering silicon carbide for enhanced borders and ports security

NATO OTAN

This activity is supported by:

The NATO **Science** for **Peace** and **Security** Programme

Particle detection (IBIC spectra) - partly damaged 4H-SiC SBD detector

Short probe

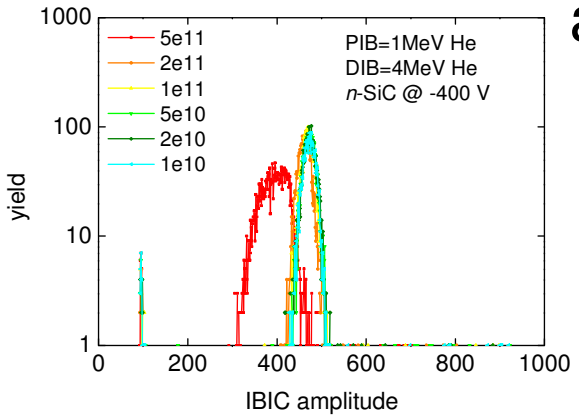

Same probe

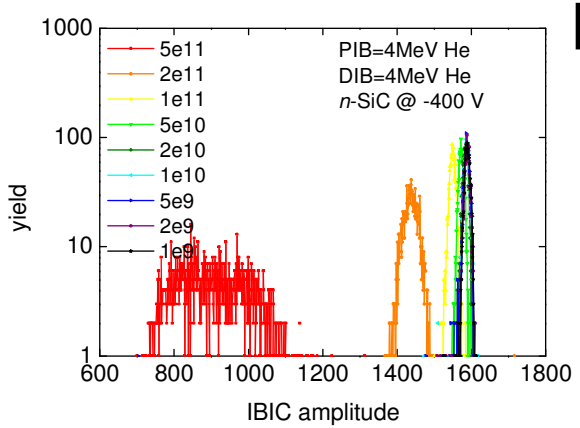

Long probe

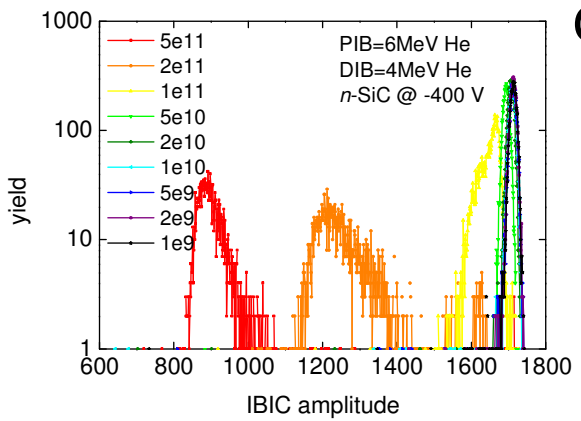

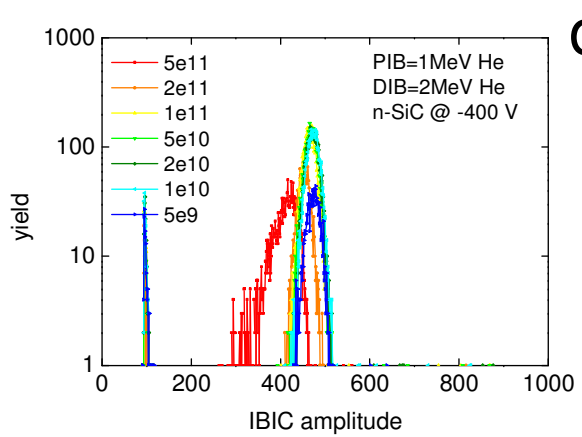

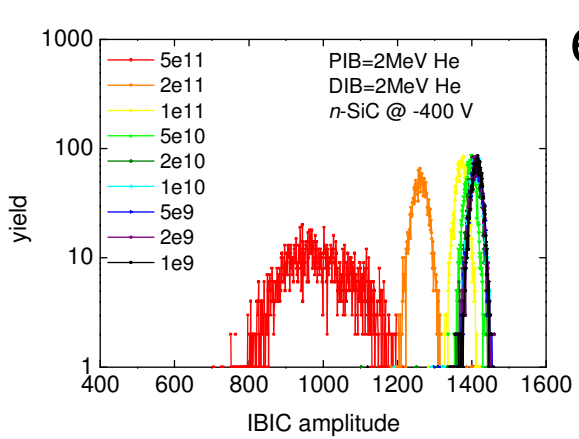

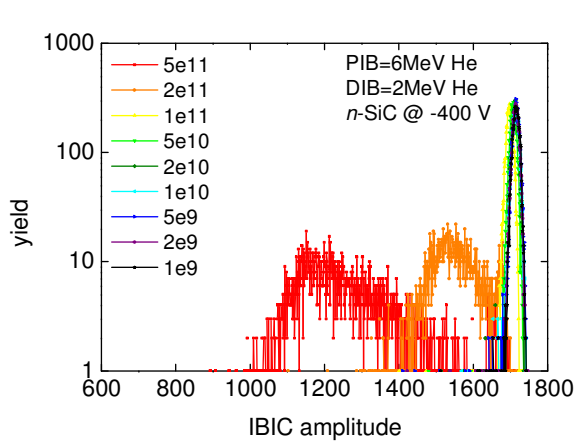

IBIC spectra obtained for detection of (a, d) 1 MeV He, (e) 2 MeV He, (b) 4 MeV He, (c, f) 6 MeV He ions (PIB) using two partly damaged 4H-SiC SBDs damaged with 4 MeV He (a-c) and 2 MeV He ions (DIB) (d-f); bias = -400V for all.

Case A: 4H-SiC – shallow damage – 2 MeV He

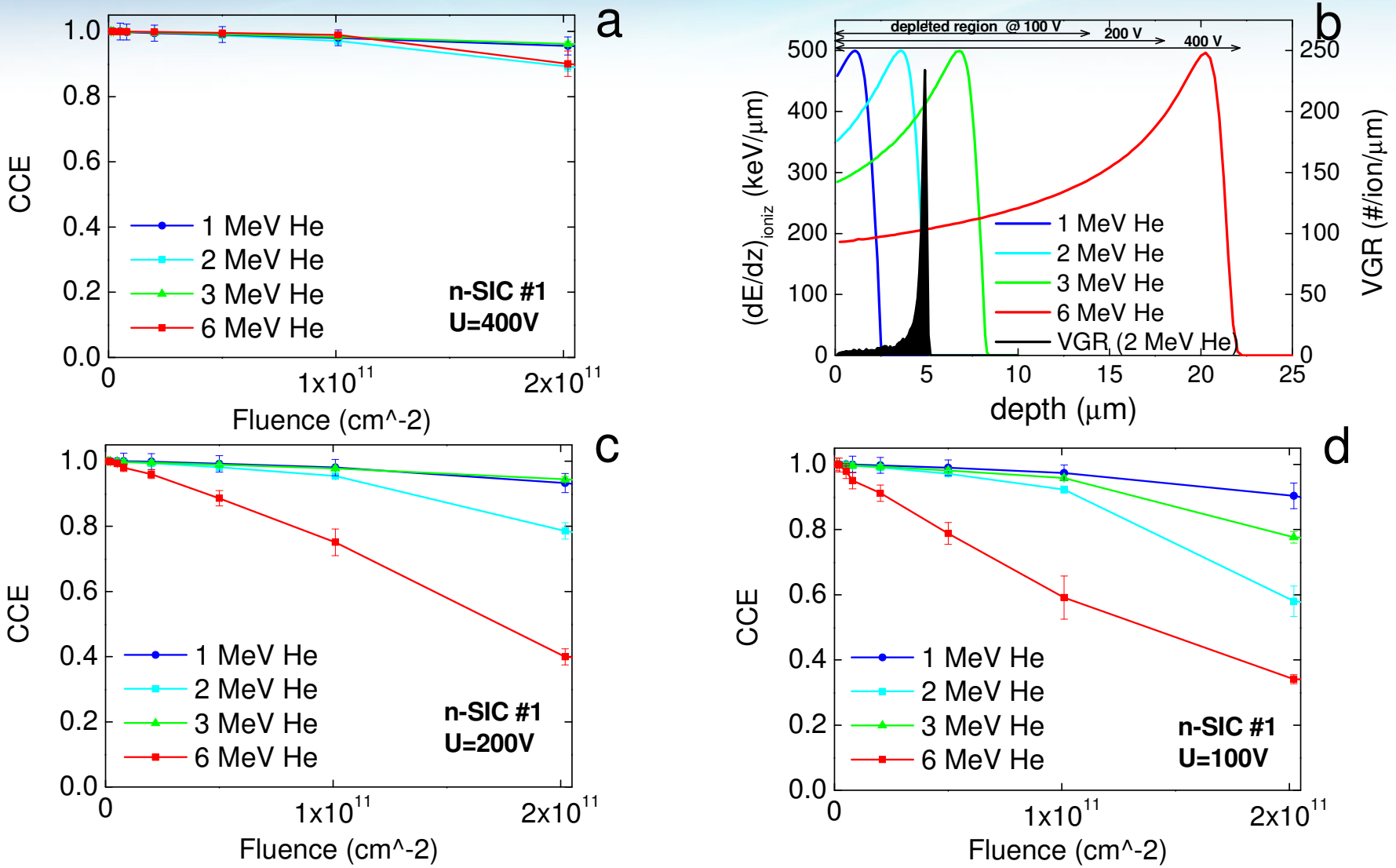

Calculated CCE value degradation distributions for detection of various probing ions (PIB) using the same pattern irradiated and partly damaged 4H-SiC SBD (#1: DIB = 2 MeV He) for biases: (a) -400 V, (c) -200 V and (d) -100 V.

Case B: 4H-SiC – deep damage – 4 MeV He

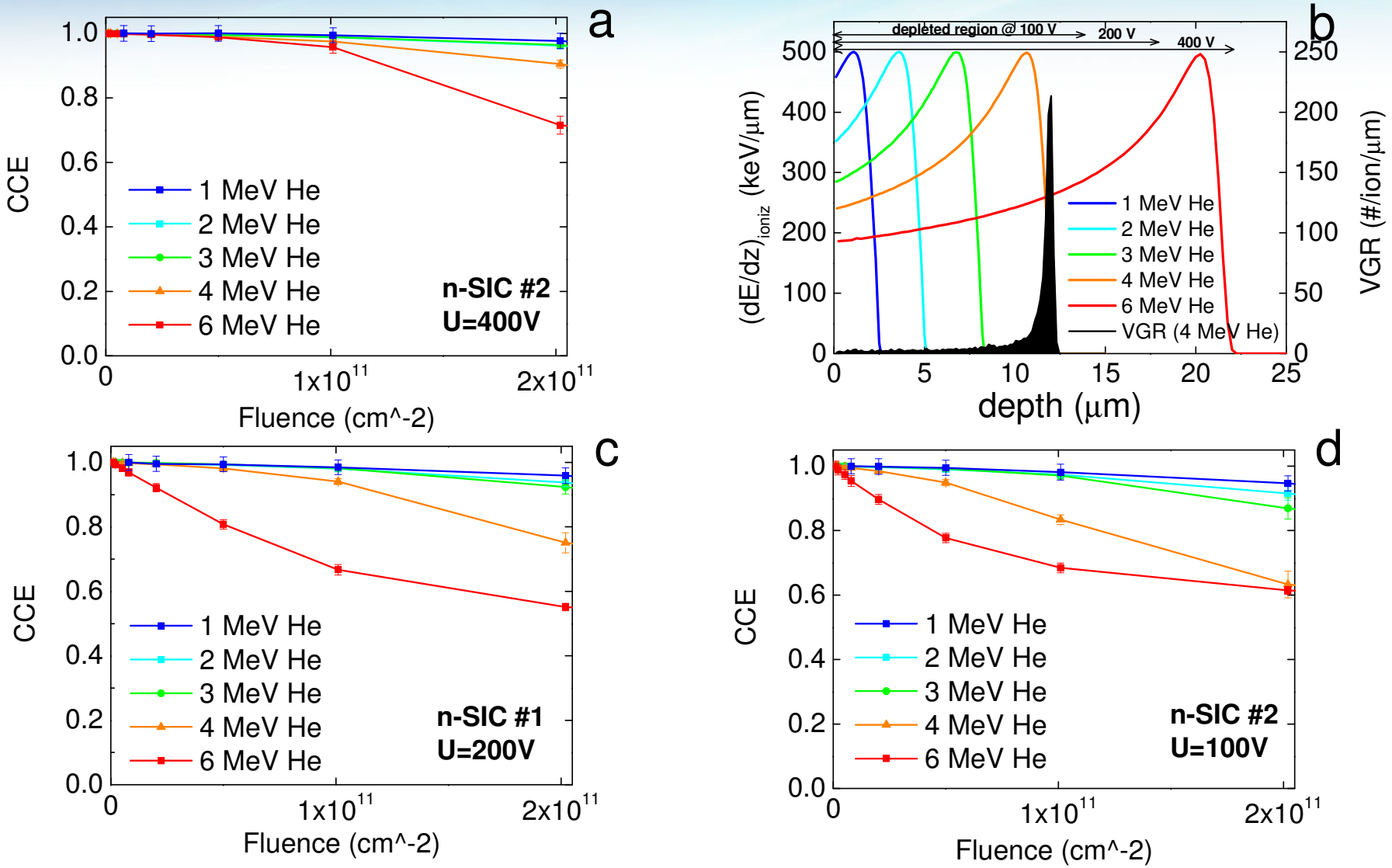

Calculated CCE value degradation distributions for detection of various probing ions (PIB) using the same pattern irradiated and partly damaged 4H-SiC SBD (DIB = 4 MeV He for biases: (a) -400 V, (c) -200 V and (d) -100 V.

Defect analysis: Deep Level Transient Spectroscopy

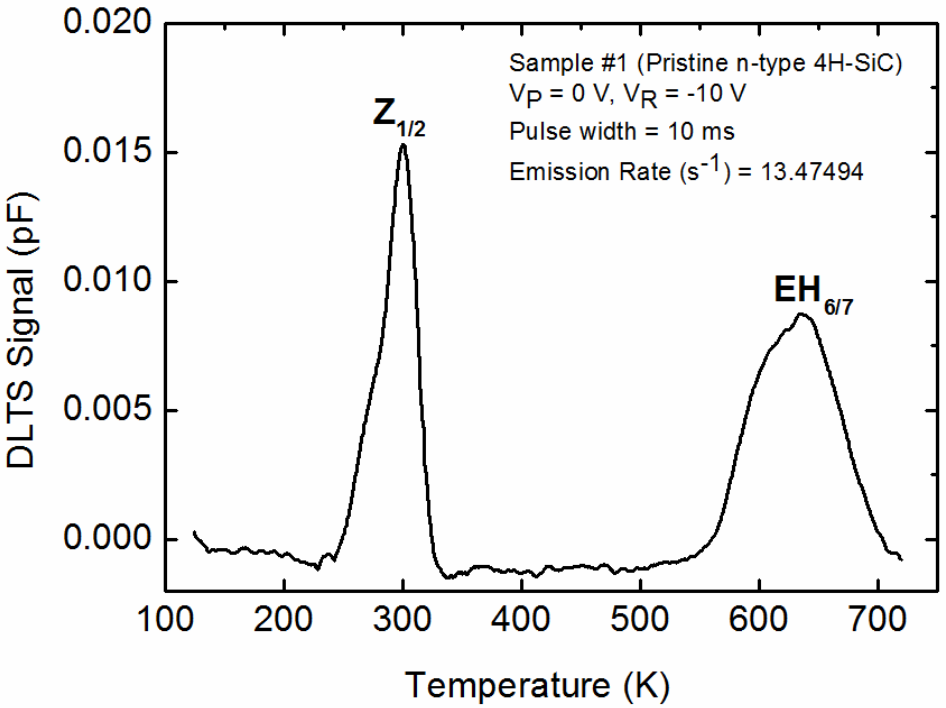

DLTS spectra of the pristine (#1) SBD sample measured at the maximum reverse bias voltage of -10 V, the pulse height of 10V, the pulse width of 10 ms and emission rate of 13.47 s-1.

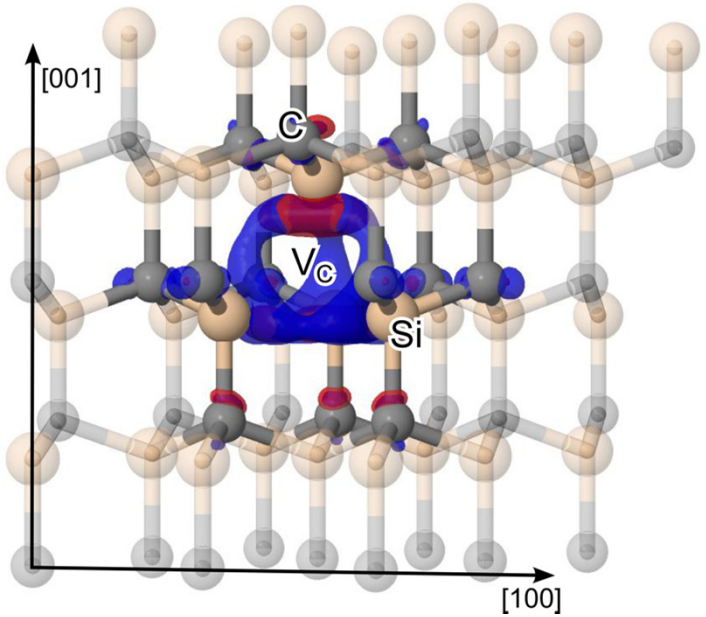

Trap	E_t (eV)	σ (cm^{-2})	Attribution
$Z_{1/2}$	0.64	3×10^{-15}	Vc(=/0)
$EH_{6/7}$	1.84	1×10^{-12}	V_c(0/+)

Two deep level centres $Z_{1/2}$ and $EH_{6/7}$ found, corresponding to two charge states of the carbon vacancy.

Defect analysis of the implanted sample (#2): Deep Level Transient Spectroscopy

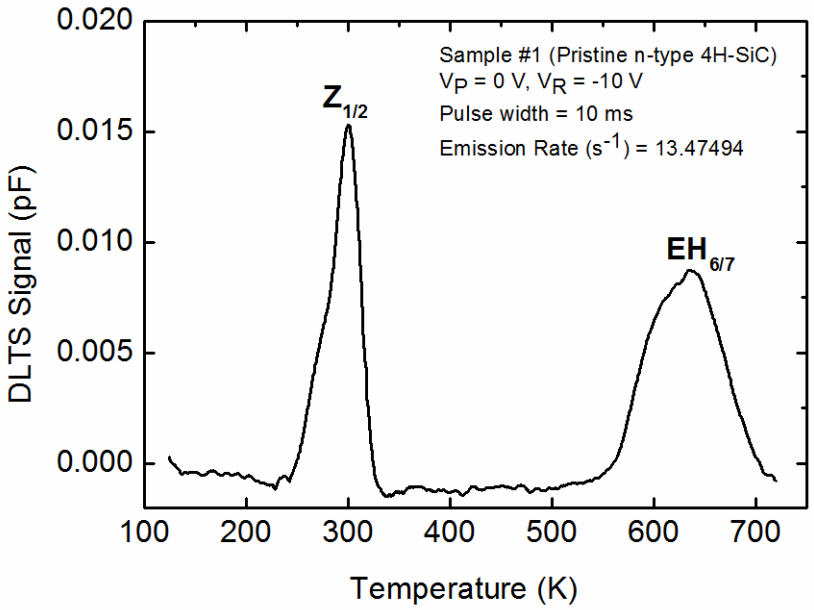

DLTS spectrum of the pristine sample #1.

2 MeV He

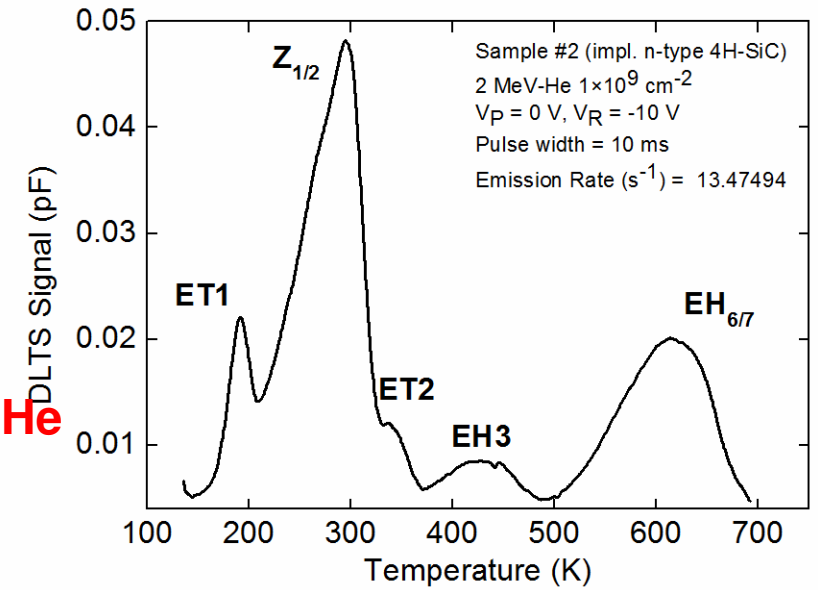

Formation of additional deep level centres (E1, ET2, and EH3) in implanted sample #2 (with 2 MeV He ions).

Trap	E_t (eV)	σ (cm^{-2})	Attribution
ET1	0.35	1×10^{-16}	Unknown*
$Z_{1/2}$	0.64	3×10^{-15}	Vc(=/0)
ET2	0.65	9×10^{-17}	Intrinsic**
EH3	1.06	4×10^{-14}	Intrinsic***
$EH_{6/7}$	1.84	1×10^{-12}	V_c(0/+)

Free carrier concentration decrease in implanted samples

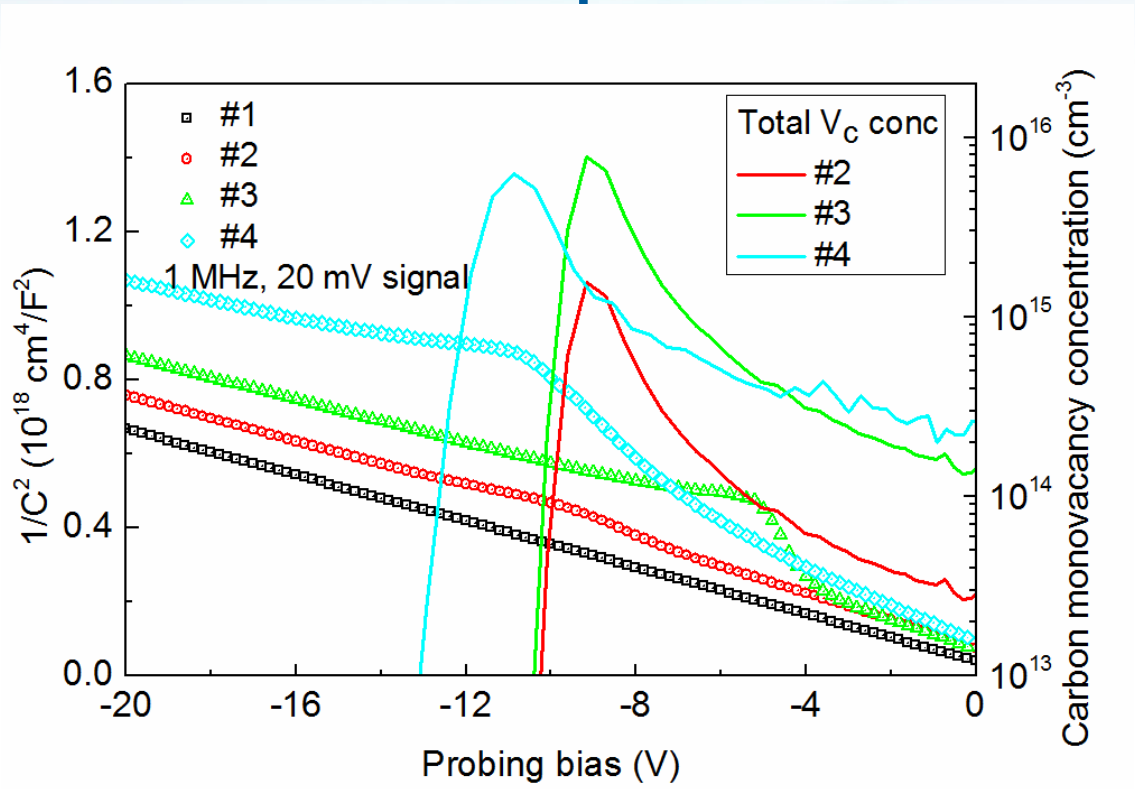

Results of 1 MHz C-V measurements for the pristine sample #1 (black squares), 2 MeV He implanted samples #2 (red circles), #3 (green up triangles), and 600 keV H implanted sample #4 (cyan rotated squares) are combined with simulated total carbon vacancy concentration distributions (lines) following implantation of the selected SBD devices with 2 MeV He ions for fluence values of 1e9 cm-2 (#2), 5e9 cm-2 (#3), and with 600 keV H ions up to fluence value of 5e10 cm-2 (#4).

Change in doping profile directly corresponds to primary defect profile – deep level defects are formed from vacancies and interstitials in ion cascades.

Ion fluence increase → [ET2] & [EH3] increase

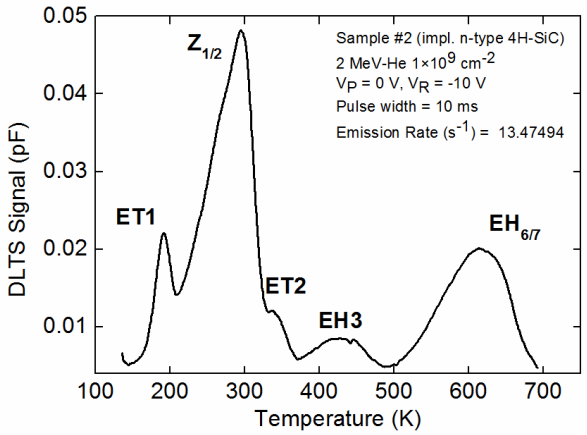

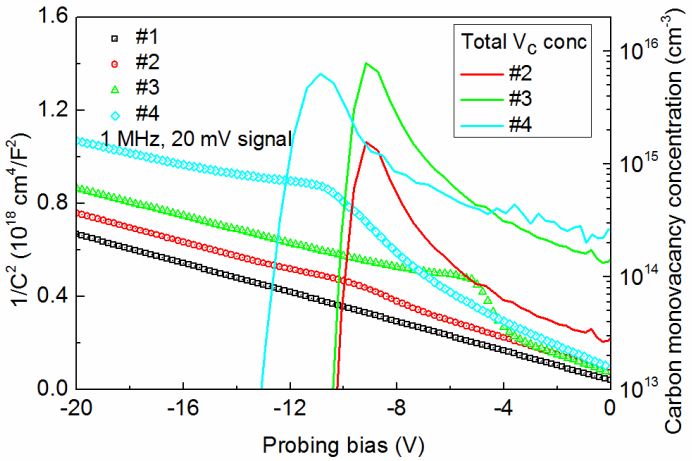

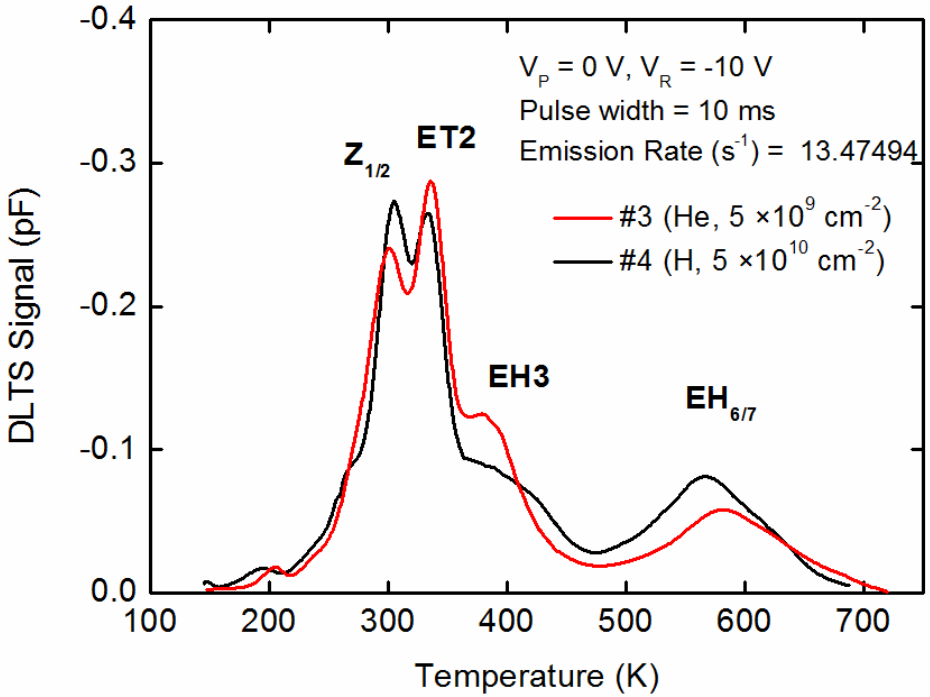

DLTS spectra obtained for samples implanted with He ions (#3) and H ions (#4), for the reverse bias of -10 V, the filling pulse of 0 V, 10 ms pulse width, and the emission rate of 13.47 s-1. The spectra are recorded during the annealing to 700K for the first time.

Ratio of ET2 to Z1/2 increases.

Low temperature annealing → ~~ET1 & ET2~~

AFTER

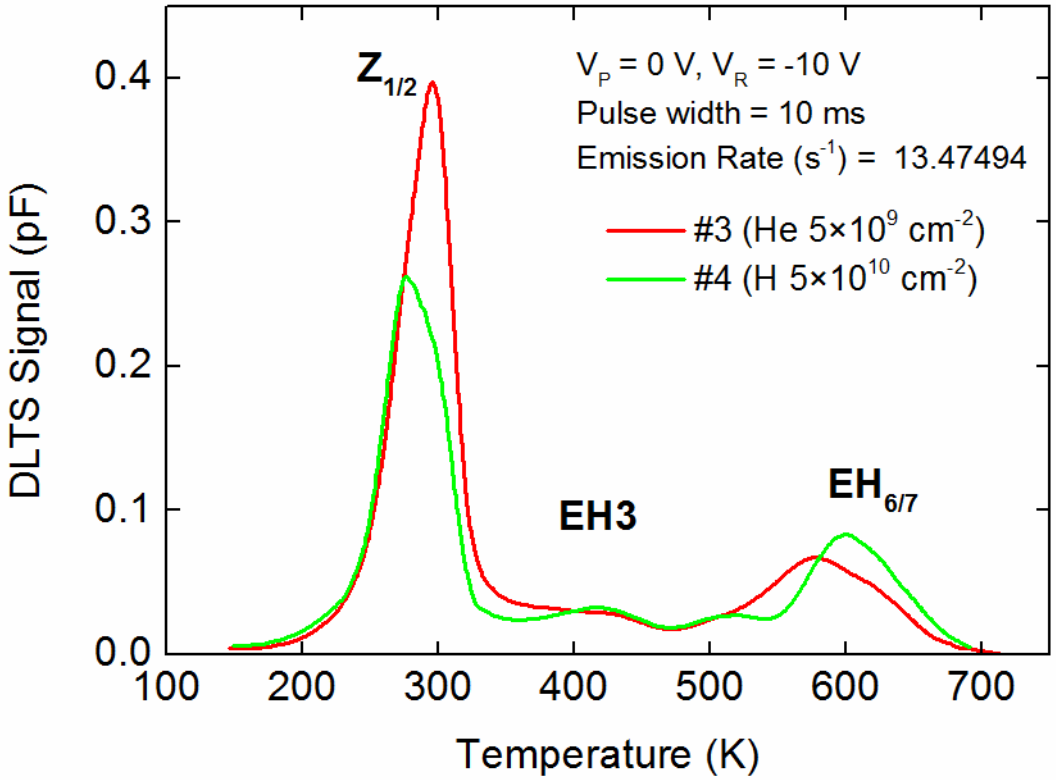

DLTS spectra recorded during the second temperature scan after the low temperature annealing of samples implanted with 2 MeV He (#3) and 600 keV (#4), for the reverse bias of -10 V, the filling pulse of 0 V, 10 ms pulse width, and the emission rate of 13.47 s-1.

BEFORE

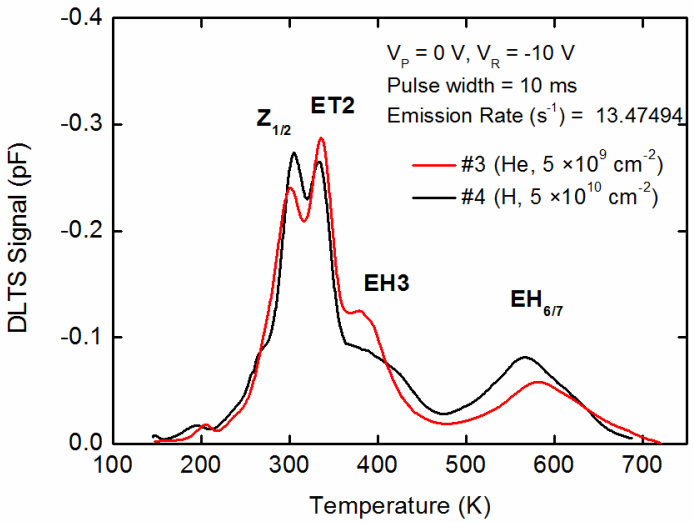

ET1 and ET2 deep level centres are annealed out.

$Z_{1/2}$ is likely to be annealing product of either ET1 or ET2.

Low temperature annealing → ~~ET1 & ET2~~

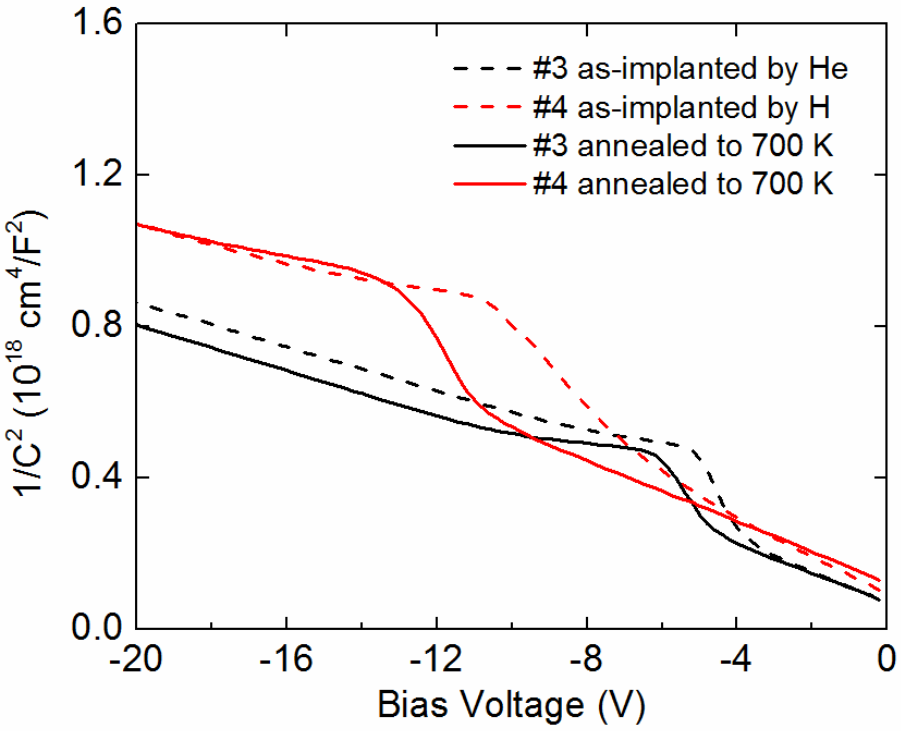

1/C2 vs. V characteristics for the samples #3 and #4 before (dashed lines) and after (solid lines) low temperature annealing up to 700K.

Net free carrier concentration partial recovery following the low temperature annealing.

BEFORE

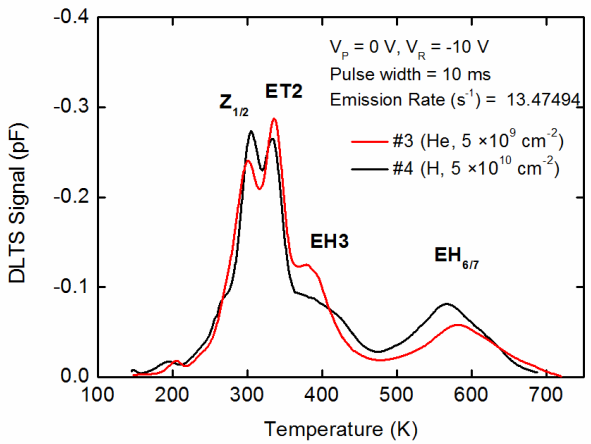

AFTER

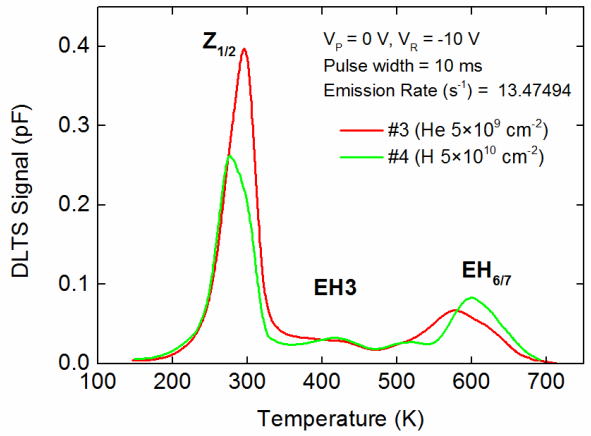

Preliminary conclusions

- Formation of defects ET1 (0.35 eV), ET2 (0.65 eV) and EH3 (1.06 eV) which have been clearly distinguished from the presence of the dominant carbon vacancies ($Z_{1/2}$ and $EH_{6/7}$) in increased concentrations after implantation of either H or He ions.

- Strong increase in ET2 concentration compared to $Z_{1/2}$ concentration with the fluence, using the standard DLTS set-up and without any post implantation treatment, which has not yet been observed or reported in literature, in both cases of H and He ion implantation in the single ion regime.

- Low temperature annealing up to 700 K revealed the almost complete removal of ET2 and ET1 traps, and the partial removal of EH3 trap, while the concentrations of $Z_{1/2}$ and $EH_{6/7}$ traps have further increased.

- The ET2 and EH3 defects: i) act as majority carrier removal traps, ii) exhibit a low thermal stability and iii) can be related to the simple point-like defects introduced by light ion implantation, namely interstitials and/or complex of interstitials and vacancies in both carbon and silicon sub-lattices.

Acknowledgements

QST – Japan

Shin-ichiro Sato

Yuya Kumbayushi

Takeshi Ohshima

INFN & Univ. Torino – Italy

Jacopo Forneris

Paolo Olivero

Ettore Vittone

IRB – Croatia

Ivana Capan

Milko Jakšić

Tomislav Brodar

Natko Skukan

ANSTO – Australia

David Button

David Cohen

Mihail Ionescu

Shane Long

Mick Mann

Rainer Siegele

NCRIS
CAS Funding by National Collaborative Research Infrastructure Strategy

E-SiCure Project
Engineering silicon carbide for enhanced borders and ports security

This activity is supported by: The NATO **Science** for **Peace** and **Security** Programme